Climate Dynamics of Western-Central Hindu Kush Himalayas

A MS Project Report submitted in partial fulfilment of the requirements for the Award of the degree of Master of Science

By

AASADEEP SINGH

16MS013

Under the guidance of

Dr. Prasanta Sanyal

To the

DEPARTMENT OF EARTH SCIENCES

Indian Institute of Science Education and Research

Kolkata

July, 2021

Certificate

Date: 23/07/2021

This is to certify that the MS Project Report entitled **"Climate Dynamics of Western-Central Hindu Kush Himalayas"** submitted by Mr. Aasadeep Singh, Registration No. 16MS013, a student of Department of Earth Sciences of the 5 Year BS-MS Dual Degree Programme of IISER Kolkata, is based upon his own research work under my supervision. This is also to certify that neither the report nor any part of it has been submitted for any degree or any other academic award anywhere before. In my opinion, the project fulfils the requirement for the award of BS-MS Dual Degree.

Prasanta Sanyal

Dr. Prasanta Sanyal
Professor
Department of Earth Sciences,
Indian Institute of Science Education and Research Kolkata
Mohanpur, 741246, West Bengal, India

Declaration

Date: 23/07/2021

I, Mr. Aasadeep Singh, Registration No. 16MS013, a student of the Department of Earth Sciences of the 5 Year BS-MS Dual Degree Programme of IISER Kolkata, hereby declare that this MS project report is my own work and, to the best of my knowledge, it neither contains materials previously published or written by any other person, nor has it been submitted for any degree/diploma or any other academic award anywhere before. I have used the originality checking service to prevent inappropriate copying.

I also declare that all copyrighted material incorporated into this project report is in compliance with the Indian Copyright Act, 1957 (amended in 2012) and that I have received written permission from the copyright owners for my use of their work.

Aasadeep Singh

Aasadeep Singh
Department of Earth Sciences.
Indian Institute of Science Education and Research Kolkata
Mohanpur 741246, West Bengal, India

Acknowledgement

I want to take this time to convey my utmost gratitude to my research guide Dr. Prasanta Sanyal, for providing me with the chance to undertake my master's project in his lab. His guidance was vital during the research and writing of this report. I owe him a debt of gratitude for his unwavering encouragement and drive throughout the project.

I would like to thank Bibhasvata Dasgupta, one of the lab seniors and data analytically proficient who is not only my project report mentor but the one who has transformed me to be able to accomplish this work by motivating me throughout the ups and downs of my study. I can't praise him enough for taking the time and making the effort to teach me and provide solutions to my never-ending challenges.

I am appreciative for the kind help and valuable suggestions from my fellow laboratory members in SILIKA - Anurag Kumar, Deepak Jha, Vijayananda Sarangi, Santrupta Samantray, Sohom Roy, Biswajit Roy, Mahesh, Nigam, Ajay and Bibhasvata Dasgupta. I would also like thank my life savior Ajay who helped me with the coding challenges with MATLAB.

I am especially grateful to SILIKA batchmates - Mukesh & Twismary for their unwavering support throughout my time there.

I am blessed with friends like Tannu, Prince, Antonio, Soham, Rajiv, Geeta, Purnima & many others who have been a continual source of inspiration & motivation throughout.

Finally, and most significantly, I would like to express my gratitude to my family (especially my father) for their unwavering love and unwavering moral support. Their immediate guidance and support have aided me in overcoming all of the challenging hurdles I have encountered during my work.

Dedication

Dedicated to my parents, seniors, instructors, and teachers who taught me that changing career pathways to pursue your deep passion is never too late, and that context is everything.

Contents

Tables & Figures

1.

Figure 1 | Rain Hydrograph (IAEA Precipitation Dataset), DJFM & JJAS Dominated Areas

2.

Figure 2 | Study Areas – NWH, WH & TH, Generated through MATLAB of the ERA-5 dataset of Indian subcontinent

Figure 2a | Graphical representation of ITA (Source – [9])

Table 1 | Data Description (ERA-5)

Table 2 | Variables Used for Meteorological Trend Analysis

3.

Figure 3 | SCA, Sf & t2m Interpolant Temporal Plots for NWH_Annual

Figure 4 | SCA, Sf & t2m Interpolant Temporal Plots for NWH_DJFM Figure 5 | SCA, Sf & t2m Interpolant Temporal Plots for NWH_JJAS

Figure 6 | Sf & t2m Interpolant Temporal Plots for WH_Annual

Figure 7 | Sf & t2m Interpolant Temporal Plots for WH_DJFM

Figure 8 | Sf & t2m Interpolant Temporal Plots for WH_JJAS

Figure 9 | SCA, Sf & t2m Interpolant Temporal Plots for TH_Annual

Figure 10 | SCA, Sf & t2m Interpolant Temporal Plots for TH_DJFM

Figure 11 | SCA, Sf & t2m Interpolant Temporal Plots for TH_JJAS

Figure 12 | Sf Temporal Plot for NWH_Annual

Table 3 | Regression Analysis for Snowfall Vs. Years, NWH_Annual

Figure 13 | Sf Temporal Plot for NWH_DJFM

Table 4 | Regression Analysis for Snowfall Vs. Years, NWH_DJFM

Abbreviations

HKH	Hindu Kush Himalayan
NWH	North Western Himalayas
WH	Western Himalayas
TH	Tibetan Himalayas
NWH	The total study area of NWH
WH	The total study area of WH
TH	The total study area of TH
Sf	Snowfall
SCA	Snow Cover Area
t2m	Temperature
SDE	Snow Depth
STR	Surface Thermal Radiation
SSHF	Surface Solar Heat Flux
DJFM	Sum of months : December, January, February & March
JJAS	Sum of months : June, July, August & September

Abstract

The HKH region being one of the largest snow reservoir and regarded as being climatically inconsistently sensitive. The Changes in multi meteorological variables was studied for Western-Central HKH region of North-Western India using ERA-5 reanalysis monthly averaged mean data from 1979-2018 (40 years). Kendall Tau trend was calculated for monthly averaged mean data for these 40 years to define and examine the study areas. Mann-Kendall Test, Sen's Slope estimator & Innovative Trend Analysis was performed at these spatial study regions for multi-temporal scales i.e., Annual, Winter & Monsoon. Then, spearman correlation was employed to find out association of SCA with snowfall & temperature. Model fitting for climatic variables with temporal scale and among them was accomplished by regression via MATLAB. Results revealed that the there exists a significant decreasing trend of SCA in annual and monsoon scale of NWH region with a rate of 0.35%/year & 0.13%/year respectively, though temperature increased annually and during monsoon in NWH region which explain the decreasing trend in SCA. Mean winter snowfall was calculated for all 3 study areas and it was found that snowfall in NWH is highest followed by WH and then TH due to decreasing influence of Western Disturbances to southwards and eastwards. SCA trends of study area revealed that only in NWH, trend exists i.e., decreasing. Correlation Analysis revealed statistically significant negative correlation, ranging from -0.81 to -0.77 in all spatial areas w.r.t annual scale in the past 40 years and non-significant correlation value of 0.23 exists between SCA & snowfall for Monsoon period in WH. Moreover, SCA was controlled mainly by temperature and snowfall, and amount of contribution from either changes spatio-temporally, so for instance the temperature dominates in monsoon season of WH but snowfall controls more in ratio during monsoon season of TH. Modelling of parameters was employed in tools of MATLAB that revealed that the model that fits for Snowfall time series for North Western Himalayas in winter period is a Fourier series with 7 terms but for SCA and snowfall; it is linear fit in a temporal scale of same region with R^2 = 0.51 & 0.62 respectively.

1. Introduction

The Hindu Kush Himalayan region is an important mountain range of South Asia called "Water Tower of Asia" [1] and a large reservoir of snow cover, also known as third Polar Region as they play a major role in supplying water to major rivers of South Asia. It is distributed in different countries geographically like China, India, Myanmar, Afghanistan, Bhutan, Nepal & Pakistan. Snow cover is the most important parameter dealing with global energy and for atmospheric boundary layer development [2,3]. It shows strong negative correlation with surface temperature [4,5]. Therefore, it can be concluded that globally or regionally, change in snow cover area would depict climate change [6,7]. It was reported that relation between surface temperature & precipitation directly affects snow variables by Bednorz [8]. In several literatures, it had been observed that since last century, Himalayan region is warming up faster than what global average is [9, 10]. In Indian Himalayas, a decrease in snowfall with increase in surface temperature for different seasons was observed [11]. In North Western Himalayas, the SCA showed non-significant increasing trend from 2010 to 2016 [6]. The changes in snow cover were observed in different parts of HKH from 28% to 16% [12], due to changing trends of snowfall & temperature [13]. Also, some studies revealed that there are increasing trends of temperature observed due to absorption of solar radiation by soot and its deposition in snow & glaciers [14]. For HKH region, snow cover of annual scale decreased by 16% each decade from 1990 to 2001 [15]. The SCA peak is different due to influence of different weather systems. In Western Himalayas, Kashmir Valley & Qinghai-Xizang (Tibetan Plateau); the SCA peaks in February, January & March respectively. [16, 17 ,18]. Therefore it felt the need of hour to study climate dynamics of western-central HKH of specifically in North-western India with a small part of Tibetan plateau for our study. In the figure, We can see different locations having influence from JJAS and some from DJFM, and we can clearly observe the Precipitation dynamics of the this particular Hindu Kush Himalayan region, the climatic uncertainty of this particular HKH region. The HKH region's ecosystems are diversified due to the region's diverse climatic conditions. But the climate dynamics of a great part of western-central HKH, especially in North Western India are greatly influenced by Western Disturbances in winter period. It receives 1/3rd of its yearly precipitation from Western Disturbances and so how the temperature is changing here at this north western part of India could be an interesting idea to look upon, so different temperature trends were observed by Kendall tau's estimation spatial plot for 3 different regions of North Western part of India. And that's why, such 3 identified spatial-temporal regions explicitly from North Western Himalayas, Western Himalayas & Tibetan Himalayas were taken into consideration for further studies and multi parameter with multi spatial-temporal analysis. This study specifically finds out the association of SCA with climatic variables, such as radiation, snowfall and temperature on a spatial-temporal variation during the year 1979-2018 using ERA-5 dataset. Trend Analysis was calculated using Mann-Kendall test at annual, winter and monsoon scale for different spatial study regions.

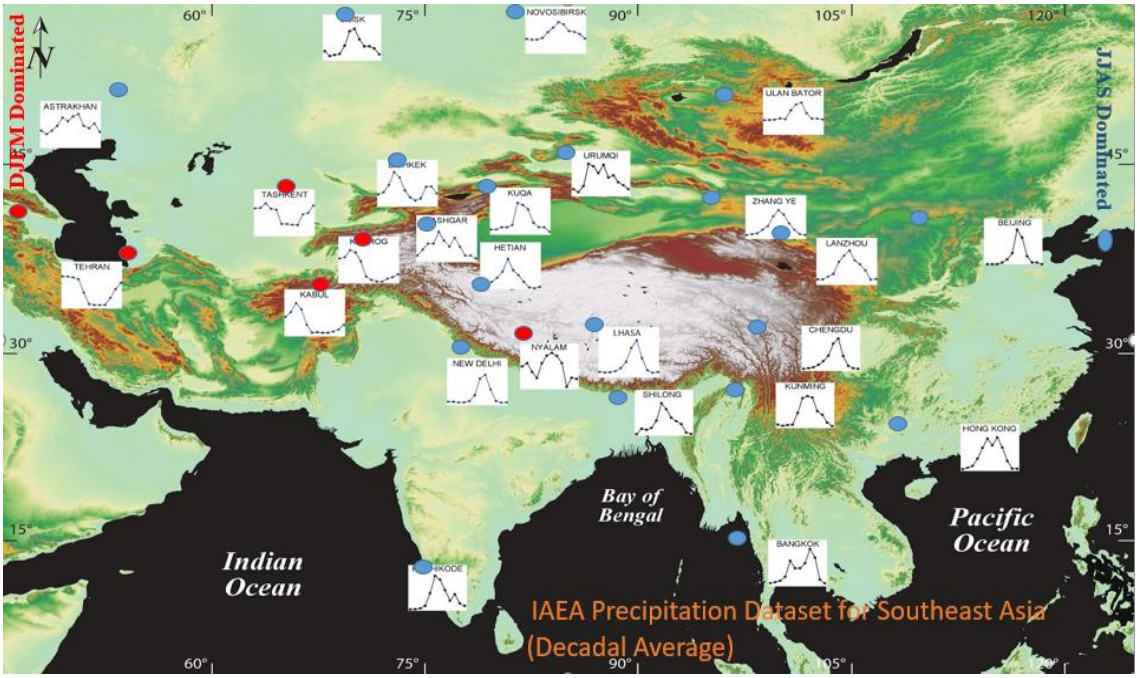

Figure 1 | Rain Hydrograph (IAEA Precipitation Dataset), DJFM & JJAS Dominated Areas

2. Data & Methodology

Traditional field methods for data collection are particularly challenging in the HKH (Hindu Kush Himalayan) region due to the enormous and mainly inaccessible locations and terrible weather conditions. Due to its synoptic and repeating coverage, satellite observations are a more viable and efficient choice, and they give a variety of products at various geographical and temporal scales. To evaluate the multiple datasets used in this work, we used the MATLAB & R programming language.

2.1. The Study Area:

The HKH region's ecosystems are diversified due to the region's diverse climatic conditions. The HKH region features large ice and snow ranges that cover around 0.76 million km^2 [19]. We have identified specific areas explicitly from NWH (North Western Himalayas), WH (Western Himalayas) & TH (Tibetan Himalayas) in Western-Central HKH region based on change in trends observed in spatial plots (**Figure 2**).

Asia has the world's largest, highest, and most densely populated mountain systems. The Himalaya, Karakoram, and Hindu-Kush mountain ranges stretch from Namcha Barwa in the east to Afghanistan's western border. This mountain system in Asia is made up of a succession of parallel and convergent ranges that make up the world's tallest mountain region. The HKH mountain range stretches over 3,500 km over Afghanistan, Pakistan, China, India, Nepal, Bhutan, Bangladesh and Myanmar, spanning about 43,00,000 km^2 [20].

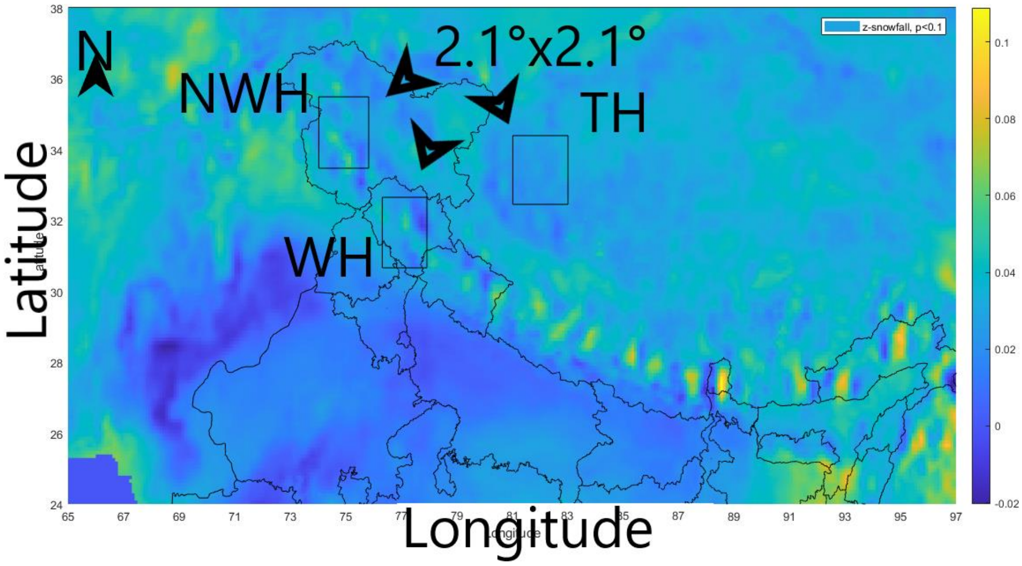

Figure 2 | Study Areas – NWH, WH & TH, Generated through MATLAB of the ERA-5 dataset of Indian subcontinent

The equal area square boxes (equal latitude-longitudinal grid) were chosen for further study inside these 3 study area boxes i.e. NWH, WH & TH where some trend change was detected (**Figure 2**).

2.2. Meteorological Dataset:

The meteorological data set was acquired from ERA5 (**Table 1**) in a .NetCDF file format where we have 40 years of monthly mean spatio-temporal data from 1979-2018 of Snowfall, Surface Temperature, Snow Cover Area, Snow Albedo, Snow Depth, Snow Depth Water Equivalent, Surface Sensible Heat flux, Surface Net Solar Radiation, Surface Net Thermal radiation of Indian Subcontinent as listed in **Table 2**.

Using the rules of physics, reanalysis combines model data with observations from around the world to create a globally complete and consistent dataset. This principle, known as data assimilation, is based on the method used by numerical weather prediction centers, in which a previous forecast is combined with newly available observations in an optimal way every so many hours (12 hours at ECMWF) to produce a new best estimate of the state of the atmosphere, known as analysis, from which an updated, improved forecast is issued.

Snow Cover Area (SCA) is estimated by Normalized Difference Snow Index (NDSI) which is determined by the ratio of the differences in VIS and SWIR reflectance; NDSI = ((band 4-band 6) / (band 4 + band 6)). A pixel with NDSI > 0.0 is considered to have some snow present. A pixel with NDSI <= 0.0 is a snow free land surface, band 4 and band 6 are just Landsat satellites numbers.

$$\text{NDSI} = \frac{\text{Reflectance}_{\text{Green}} - \text{Reflectance}_{\text{SWIR}}}{\text{Reflectance}_{\text{Green}} + \text{Reflectance}_{\text{SWIR}}}.$$

Data type	Gridded
Projection	Regular latitude-longitude grid
Horizontal coverage	Global
Horizontal resolution	Reanalysis: 0.25° x 0.25° (atmosphere) – grid box
Temporal coverage	1979 to 2018
Temporal resolution	Monthly
File format	GRIB

Table 1 | Data Description (ERA-5)

(**Source**: https://cds.climate.copernicus.eu/cdsapp#!/dataset/reanalysis-era5-single-levels-monthly-means?tab=form)

Meteorological Parameters (Variables)	Units	Description
Snowfall (Sf)	Metres of water equivalent (mwe)	It is the snow that has collected on the Earth's surface which is the summation of ***large-scale*** & ***convective snowfall.*** It is determined as mean over a particular time period which is annual mean w.r.t data extracted. m of we == metres of water equivalent which means the amount of water that is given out during melting of some 'x' amount of snow
Snow Cover Area (SCA)	%	It refers to the amount of area covered by snow at any given time in the selected grid box. SCA is calculated by Normalized Difference Snow Index (NDSI).
Snow Depth (SDE)	Meters (m)	It's the amount of snow in a grid box's snow-covered area. It's the depth at which the water would be if the snow melted equally over the entire grid box. The grid box may be completely or partially covered in snow.
2 meter Temperature (t2m)	Kelvin (K)	It is the temperature of air at a height of 2 meters over land, sea, or inland waters. This is evaluated as the annual mean based on data taken over a specific time period.
Surface Net Thermal Radiation (STR)	J/m^2	Thermal radiation, which is also called outgoing longwave radiation (OLR) released by the Earth's surface, atmosphere & clouds. It is the difference between downward and upward thermal radiation at the Earth's surface. Thermal radiation is emitted by the atmosphere, clouds & aerosols in all directions, a part of which reaches the earth as downward thermal radiation. This parameter is the annual average based on data extracted over a specific time period.

Surface Sensible Heat Flux (SSHF)	J/m^2	It is the turbulent air motion that transports heat from the Earth's surface to the atmosphere. The temperature differential between the surface and the environment, wind speed, and surface roughness all influence its amplitude. This value reflects the mean for a certain time period, which is the yearly mean based on collected data.

Table 2 | Variables Used for Meteorological Trend Analysis

(Source:https://cds.climate.copernicus.eu/cdsapp#!/dataset/reanalysis-era5-single-levels-monthly-means?tab=overview)

2.3. Statistical Analysis Methods

2.3.1. Mann-Kendall Trend Test

The Mann-Kendall (MK) test [22,23] is used to assess the statistical significance of snow cover, temperature, and precipitation patterns, and it is one of the most reliable methods for looking for persistent trends in data across time. It's a nonparametric test, which means it'll work with any distribution.

How does this test work?

- It is predicated on the null hypothesis, H_0, that there is no monotonic trend in the time series.
- Tested against 3 alternative hypothesis, i.e., a trend exists in the time series. It can be positive, negative or neither one.
    - Increasing monotonic trend
    - Decreasing monotonic trend
    - Neither an increasing nor a decreasing monotonic trend

When the 'p' value < preset significance level (α), the null hypothesis, H_0 is rejected (0.05).

Consider two subsets: X_i & X_j of the data.

where i ranges from 1,2,3 to ……n-1 & j ranges from i + 1, i + 2, i + 3 to …..n.

Mann-Kendall statistic (S) calculation/derivation:

$$S = \sum_{i=1}^{n-1} \sum_{j=i+1}^{n} \text{sign}\left(X_j - X_i\right) \qquad (1)$$

$$\text{Sign}\left(X_j - X_i\right) = \begin{cases} 1 \text{ if } X_j - X_i > 0 \\ 0 \text{ if } X_j - X_i = 0 \\ -1 \text{ if } X_j - X_i < 0 \end{cases} \qquad (2)$$

The variance (σ^2) for the S statistic is defined by:

$$\sigma^2 = \frac{n\left(n-1\right)(2n+5) - \sum_{i=1}^{m} t_i(t_i-1)\left(2t+5\right)}{18} \qquad (3)$$

The standard test statistic (Z_s) calculation/derivation:

$$Z_S = \begin{cases} \frac{S-1}{\sigma} \text{ for } S > 0 \\ 0 \text{ for } S = 0 \\ \frac{S+1}{\sigma} \text{ for } S < 0 \end{cases} \qquad (4)$$

Where;

m = number of distinct non-duplicate values,

t_i = frequency of the i^{th} term.

If $|Z_s| > Z^*(\alpha)/2$, where α is the chosen significance value, then the null hypothesis, H_0 is invalid indicating that the trend is significant. If Z>0, it shows that time series is an increasing trend, and vice versa w.r.t significance value selected at 0.05.

2.3.2. Kendall's Tau Test

It's a non-parametric measure of how closely two columns of sequential data are related [24] and a time series is a collection of events that occur in a specific order. As a result, Tau may be used to examine the relationship between time and variable Y. Because the timestamps are always growing, we may conclude there is a pattern if they are closely linked. As a result, if they are positively linked, there is an upward trend (increasing trend exists). If they are negatively linked, there is a downward tendency (decreasing trend exists).

2.3.3. Sen's Slope Estimator

Sen [25] devised a simple non-parametric technique for determining the size of a time series trend. The method used to determine the trend is as follows:

$$\beta = Median\left(\frac{x_j - x_i}{j - i}\right), \; j > i$$

where β is Sen's slope estimator. $\beta > 0$ indicates upward trend in a time series. Otherwise the data series presents downward trend during the time period. It gives the slope of the trend.

2.3.4. Innovative Trend Analysis

Şen [26] provided an innovative trend analysis. This technique is summarized in this way:

It starts with dividing the whole time series into two equal halves. Calculate Y_1 and Y_2 as the average of both halve series. Arrange the two parts of this time series in an ascending order. Plot these time series on graph while first half this lies on abscissa (x-axis) and the second half lies on the ordinate (y-axis).Then draw the y=x line on the same plot. The relative placement of the scatter point with regardd to the y=x line determines the trend. The trend is monotonically increasing if all of the points are above the y=x line; and if all of the points are below the y=x line, the trend is monotonically decreasing [27].

Its trend is computed in this way:

$$s = \frac{2\left(\overline{Y_2} - \overline{Y_1}\right)}{n}$$

The ITA trend detection procedure is depicted in Figure 3.

Figure 3 displays a 1:1 line on either axis with the first and second halves of the time series. The graph depicts events of low, moderate, and high magnitude. The magnitude event trends may be clearly recognised from the displayed data. In this approach, creative trend analysis differs from non-parametric testing in that non-parametric tests only disclose monotonic trends. As seen in Fig. 3, low-magnitude events have no trend, but moderate-magnitude events have a substantial negative trend and high-magnitude events have a slight positive trend.

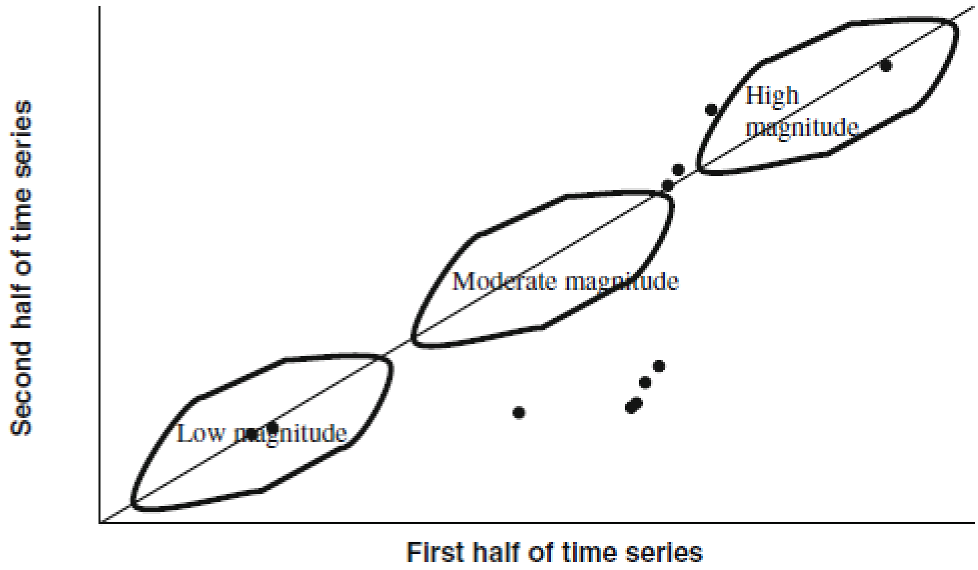

Figure 2a | Graphical representation of ITA (Source – [9])

2.3.5. Spearman & Pearson Correlation Method

Pearson correlation test checks for linearity**.** When both variables have a normal distribution that can be measured using traditional approaches like Pearson's correlation, calculating the correlation between them is simple. The rank correlation technique is preferable for nonparametric or non-Gaussian distributions. This technique transforms the data into rank data, assigns an integer rank value to each variable, and then calculates the correlation coefficient between the two ranked variables. It was assumed in this investigation that the variables have a monotonic relationship, Spearman's correlation method [28] was used to evaluate the significance of the interrelationship between SCA, Sf and t2m at the 0.05 significance level.

2.3.6. Regression Analysis

Regression Analysis is a set of statistical parameters for determining the relationship between dependent & independent variables. Two ways of fitting the model by regression modelling, one is linear regression; where one fits the line that most closely fits the data w.r.t statistical parameters of regression, for instance the method of ordinary least squares (OLS) computes a unique linear fit (or, line) that minimizes the sum of squared differences between the observed values and the predicted values (i.e., line). In Non-linear regression, observed data is modeled by a function which is a non-linear combination of model parameters/coefficients of variables and it depends on one or more independent variables. This is fitted by a method of successive approximations. The goal of this model is to make sum of the squares as small as possible.

To evaluate the goodness of fit, after trying out more than 2 models, the initial step should be to look at the fitted curve that has been showed in the MATLAB Cftool. In addition, the toolbox also provides these methods to evaluate how good the fit is for linear and non-linear parameter fits; discussed as follows:

How good the fit is? (Statistical parameters), Residual analysis, Confidence limits and predictions.

In statistical literature, accuracy of fit model has many meanings here: “good fit” can be a model.

- Taking into account the adjusted least squares assumption, the data can reasonably come from this model.
- The model coefficients can be calculated with a high degree of confidence.
- Can accurately anticipate fresh observations and explains a substantial portion of the variability in the data.

Other features of model fitting may be specified by specific applications. As a basic model, easy to describe, fitting is highly essential. All of these techniques may be used to determine how good the fit is by using the method outlined here.

There are two types of methods: graphics and numbers. Calculating good fit statistics and confidence limits of coefficients provide numerical metrics that assist statistical thinking, whereas drawing residuals and prediction limits is a graphical technique that aids visual understanding. However, graphical measurements are preferable to numeric measures since they allow you to examine the full data set at once and highlight the model's overall connection with the data. Numerical measurements concentrate on certain elements of data and frequently try to condense this information into a single number. In reality, it may be necessary to employ both types at the same time to identify the optimum match, depending on the data and analytic requirements.

It should be noted that the setting may not match the data if these techniques are used. It may be necessary to select a different model in this instance. It's also conceivable that all of the good fit metrics point to a specific fit being suitable. The resultant coefficients will be meaningless if the aim is to obtain physically relevant fit coefficients but the model does not represent the physical features of the data. In such scenario, knowing what the data means and how it's assessed is just as crucial as determining the how good is the fit.

2.3.6.1. Goodness-of-fit statistics

It is necessary to verify the good fit statistics after assessing the excellent fit using the graphical technique. For parametric models, the Curve Fitting Toolbox programme offers the following good fit statistics:

- **Sum squared error (SSE)**
- **R^2**
- **Adjusted R^2**
- **Root Mean Square Error (RMSE)**

Sum of Squares due to errors (SSE)

It's also known as the sum of squares of residuals, and it's abbreviated as SSE. The total deviation of the observed value from the fit to the observed value is calculated by this statistical measure.

$$SSE = \sum_{i=1}^{n} w_i (y_i - \hat{y}_i)^2$$

A value around 0 indicates that the model has a reduced random error component, and therefore, the fitting is better for prediction.

R^2 (R_Square)

The ratio between the regression sum of squares (SSR) and the total sum of squares

(SST) is known as R^2. The success of the fit in understanding data changes is measured by this statistical measure. R^2 is the square of the correlation between the observed value and the predicted value.

The term 'SSR' is characterized as

$$SSR = \sum_{i=1}^{n} w_i\left(\widehat{y}_i - \overline{y}\right)^2$$

SST is also known as the mean sum of squares,
& it is expressed as

$$SST = \sum_{i=1}^{n} w_i(y_i - \overline{y})^2$$

Where, SSR + SSE = SST
Therefore, R^2 can be derived and can be formulated as:

$$\text{R-square} = \frac{SSR}{SST} = 1 - \frac{SSE}{SST}$$

The value of R^2 might be any number between 0 & 1. The higher the variation described by the model, the closest the value is to 1. An R^2 score of 0.8234, for instance, indicates that the fit can explain 82.34% of the total variance in the data from the mean.

R^2 increases as the number of fit parameters in the model are increased, even if the fit does not improve in a real manner. To avoid this, modify the R^2 estimate using the degrees of freedom.

It should be highlighted that a negative R^2 can be produced for equations that do not have a constant component. Because R^2 is defined as the percentage of variation explained by the fit, it is negative if the fit is worse than simply fitting a horizontal line. R^2 cannot be regarded as the square of the correlation in this situation. This situation necessitates the addition of a constant term to the model.

Adjusted degrees of freedom R-square

This statistical measure applies the previously determined R^2 estimate to the remaining degrees of freedom and modifies it accordingly. The number of observed values, n minus the number of fitting coefficients calculated from the observed value m, is the residual degree of freedom; v = n-m.

To compute the sum of squares, v = the quantity of independent information involving n data points that is necessary.

Root Mean Squared Error

The standard error of fit and the standard error of regression are two different expressions for the same statistical measure. It is defined as the standard deviation of the random component, as follows:

$$RMSE = s = \sqrt{MSE}$$

$$MSE = \frac{SSE}{v}$$

Where, *MSE* is called mean square error;

In the same way as SSE indicates a better fit for prediction if values closer to 0, a MSE score closer to 0 indicates a better fit for prediction as well.

Important Points to note:-

Pearson & spearman correlation should be calculated to decide the model fit.

R^2 values > 0.5; are considered acceptable. R^2 adjusted, if it decreases with increasing coefficients, such models should not be considered, they are not a good fit.

The R^2 (multiple correlation coefficient of determination) indicates how much of the variance in the dependent variable can be explained by the independent variable.

- $R^2 < 0$;
    - Seen as none, in this case y = mean value; explains the variability of observed values from predicted better.
- $0.3 < R^2 < 0.5$;

    - believed to have a small/weak effect size
- $0.5 < R^2 < 0.7$;
    - Believed to have a Moderate effect size
- $R^2 > 0.7$;
    - Believed to have a strong effect size.

2.4. Procedure/Methodology

The steps below explains the data processing of the spatio-temporal data of Indian subcontinent.

1. The spatio-temporal data of Indian subcontinent for various meteorological variables was in .GRIB format which was converted to .NetCDF format using the CDO tool on Linux via the bash terminal.
2. The .NetCDF file was processed in MATLAB programming language.
3. Then Kendall tau of all variables were calculated for each pixel (latitude/longitude) for monthly averaged of 40 years and then Spearman correlations of SCA with t2m and Sf were also estimated.
4. Appropriate square boxes were selected to fix the study areas filtering this spatial data in MATLAB for further analysis where significant Kendall tau values were observed.
5. With those study areas of 3 locations i.e. NWH, WH & TH, box average was estimated followed by converting them into 3 temporal scales Yearly, DJFM & JJAS average for all variables on a yearly basis.
6. Curve Fitting Tool in MATLAB was employed for Regression Analysis of each variable at these 3 study areas for all 3 temporal scales.
7. Then the variables with these 3 temporal scales were extracted as .csv format (40 yearly average data points) from MATLAB. Mann-Kendall Trend Test with Sen’s slope estimator & Innovative Trend Analysis was estimated in R.

2.5. The Codes

The programming languages used is MATLAB & R. Essential libraries/functions used are:

- *CDO* Tool in Bash Terminal to convert .GRIB to .NetCDF format.
    - MATLAB
        - *ncread* library to read, extract and process .NetCDF variable matrix data.
        - *ktaub* function for Kendall tau b test.
        - *corr* function for calculating spearman correlation
        - *shaperead* & *mapshow* library to plot Indian boundary on spatial heat trend plots.
        - *cftool* for regression analysis.
    - R libraries
        - mk.test for Mann Kendall Test.
        - sens.slope for Sen's Slope Estimator
        - innovtrend For Innovative Trend Analysis.

3. Results

3.1. Plots of Sf, SCA & t2m

3.1.1. Interpolant plots

3.1.1.1. NWH Region

Annual

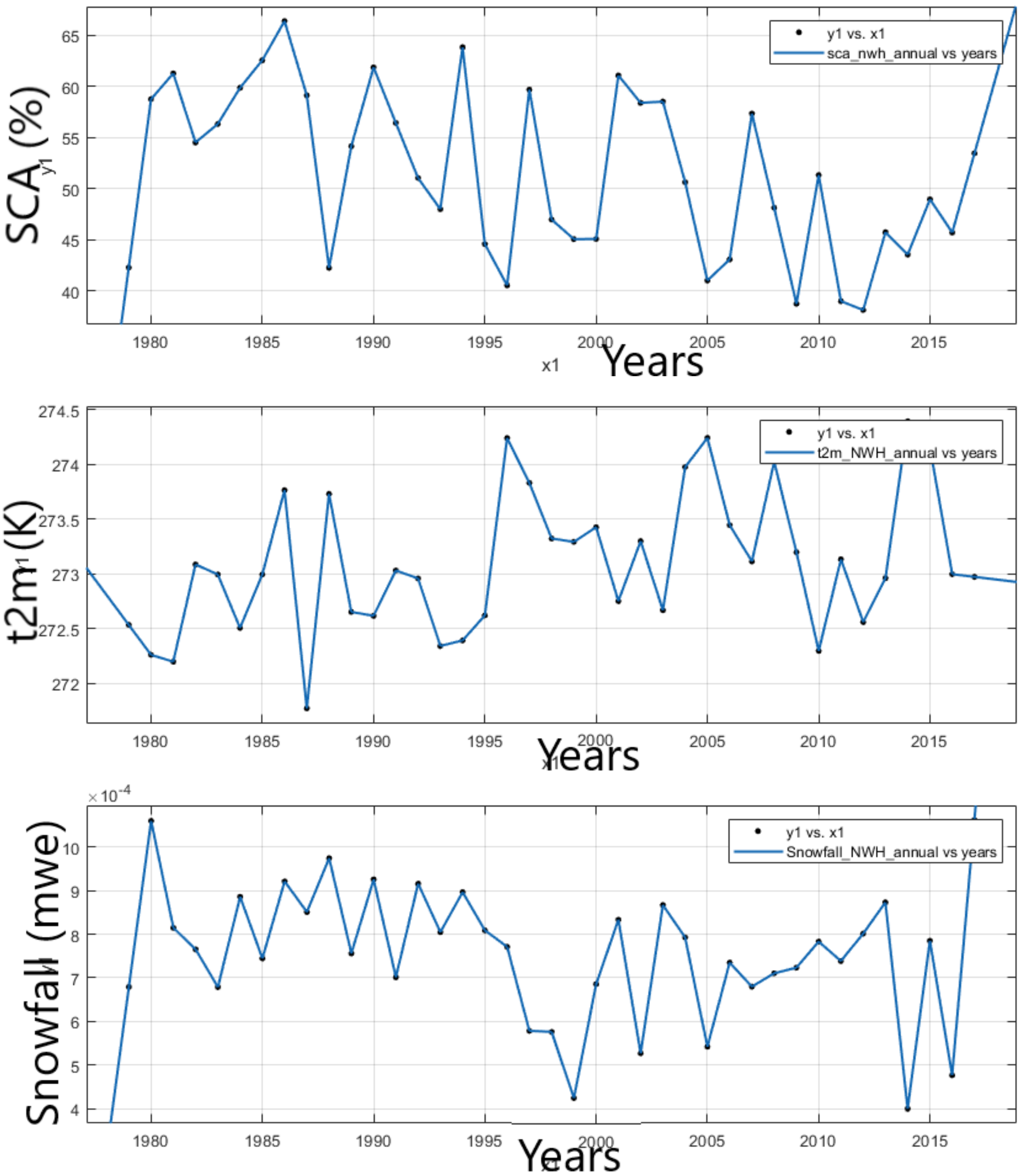

Figure 3 | SCA, Sf & t2m Interpolant Temporal Plots for NWH_Annual

DJFM

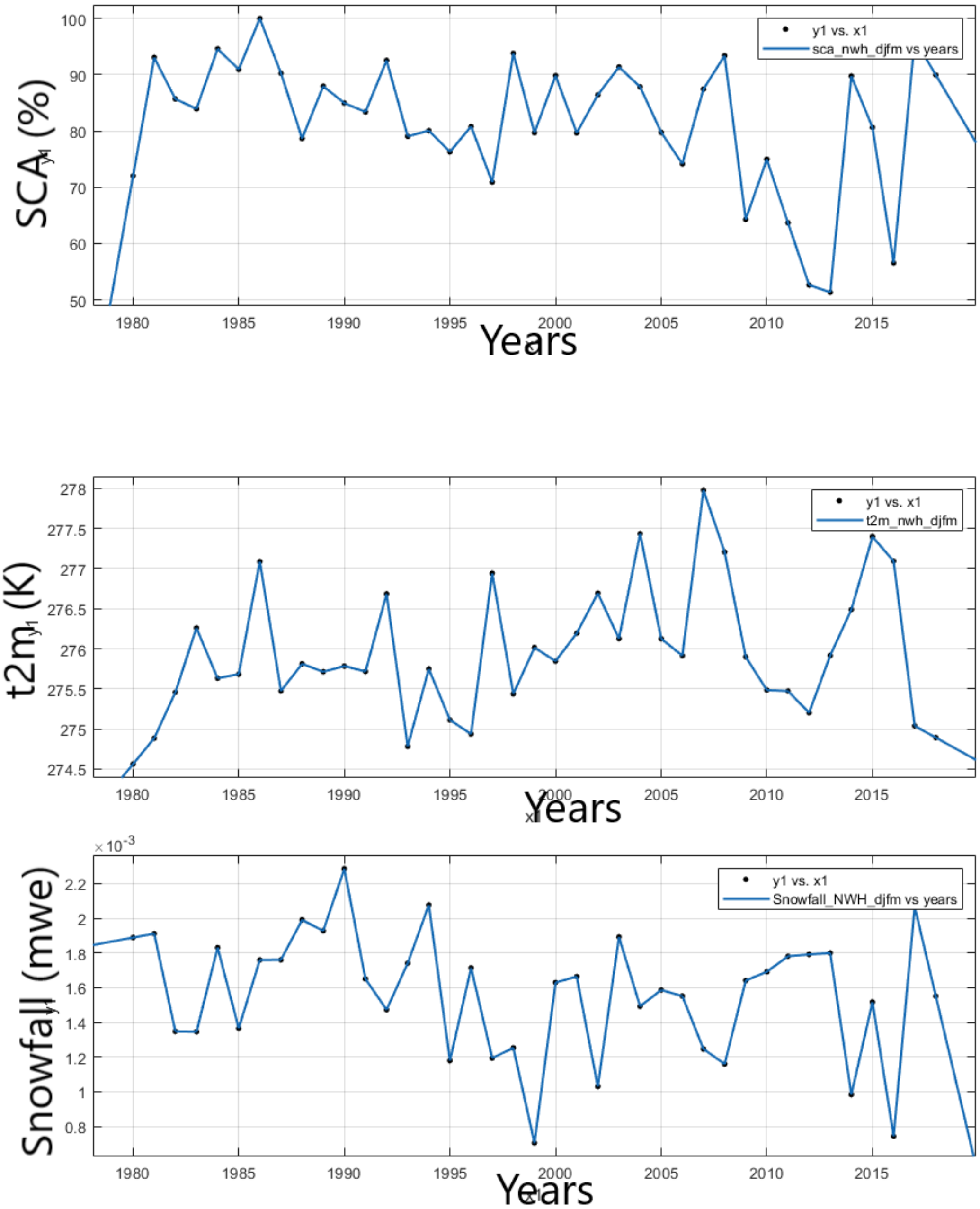

Figure 4 | SCA, Sf & t2m Interpolant Temporal Plots for NWH_DJFM

JJAS

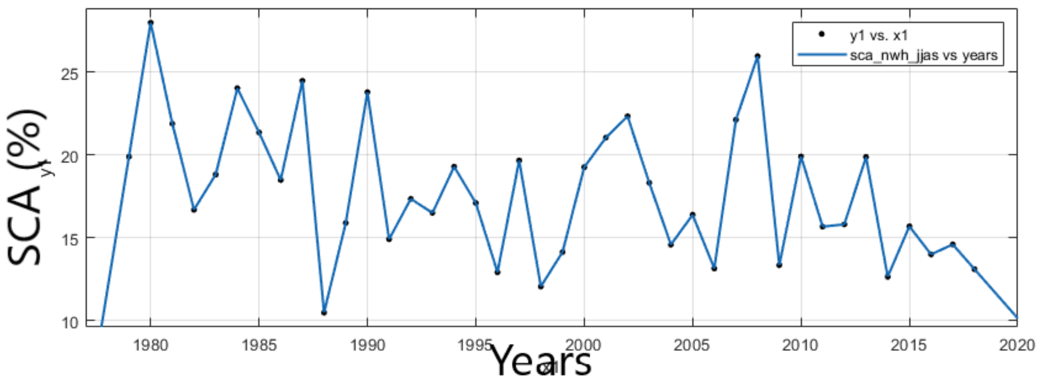

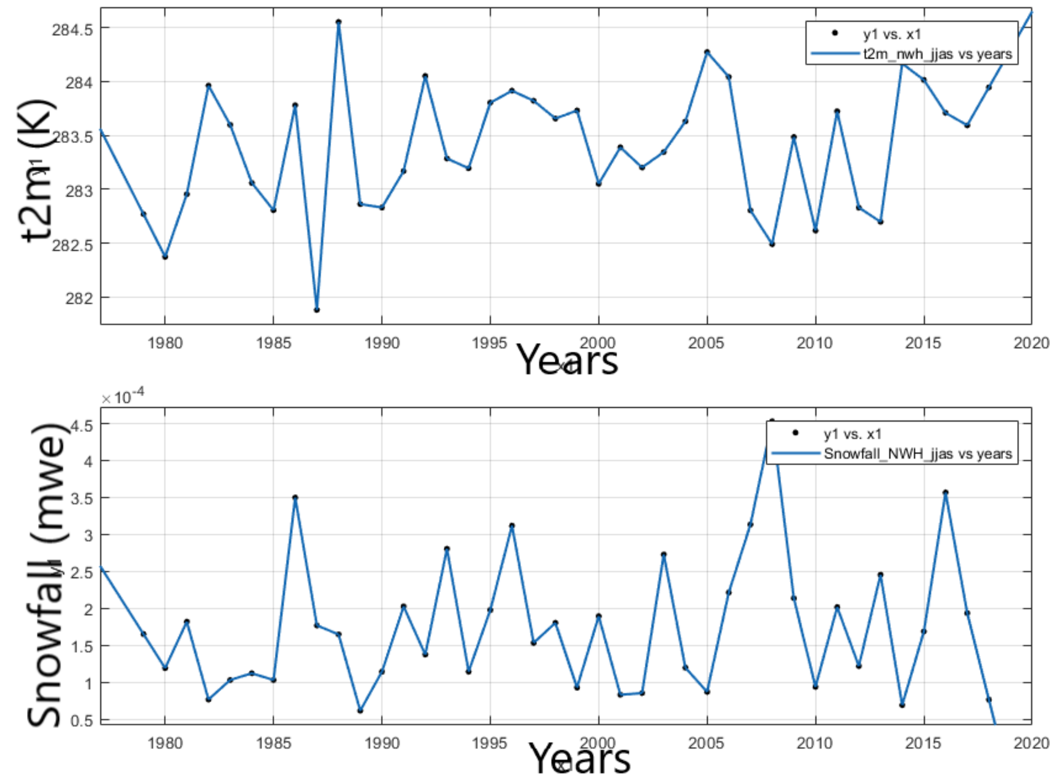

Figure 5 | SCA, Sf & t2m Interpolant Temporal Plots for NWH_JJAS

3.1.1.2. WH Region

Annual

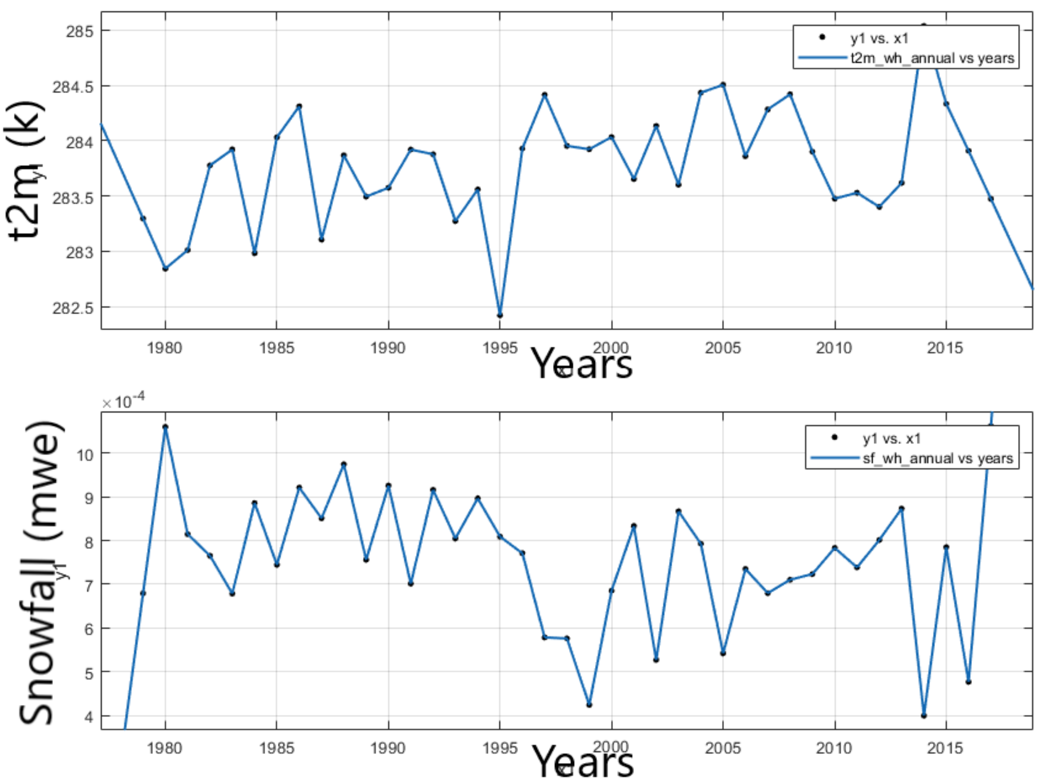

Figure 6 | Sf & t2m Interpolant Temporal Plots for WH_Annual

DJFM

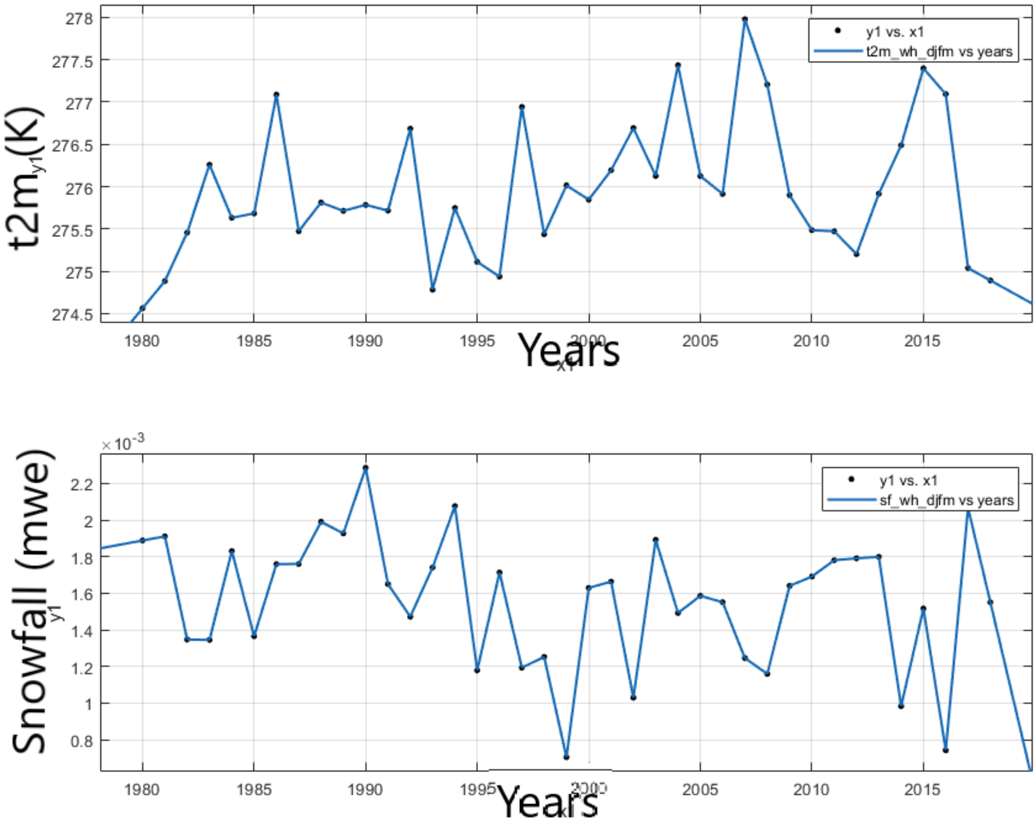

Figure 7 | Sf & t2m Interpolant Temporal Plots for WH_DJFM

JJAS

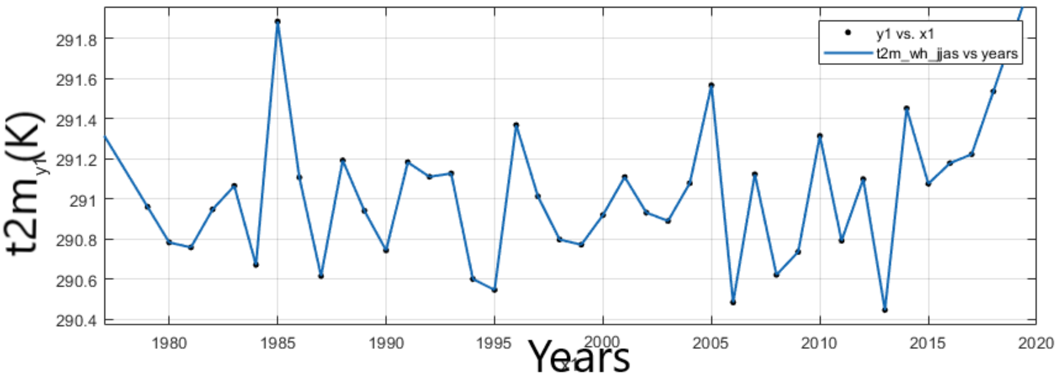

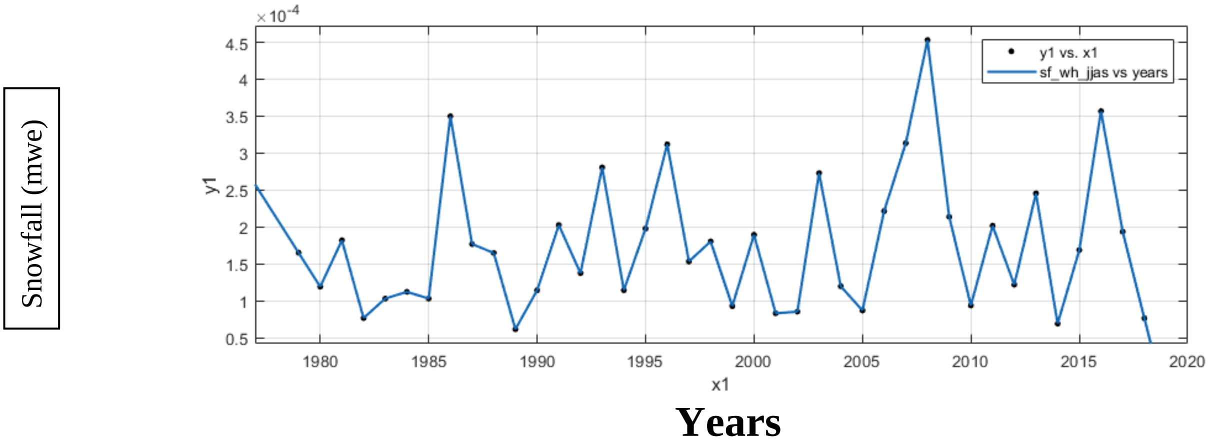

Figure 8 | Sf & t2m Interpolant Temporal Plots for WH_JJAS

3.1.1.3. TH Region

Annual

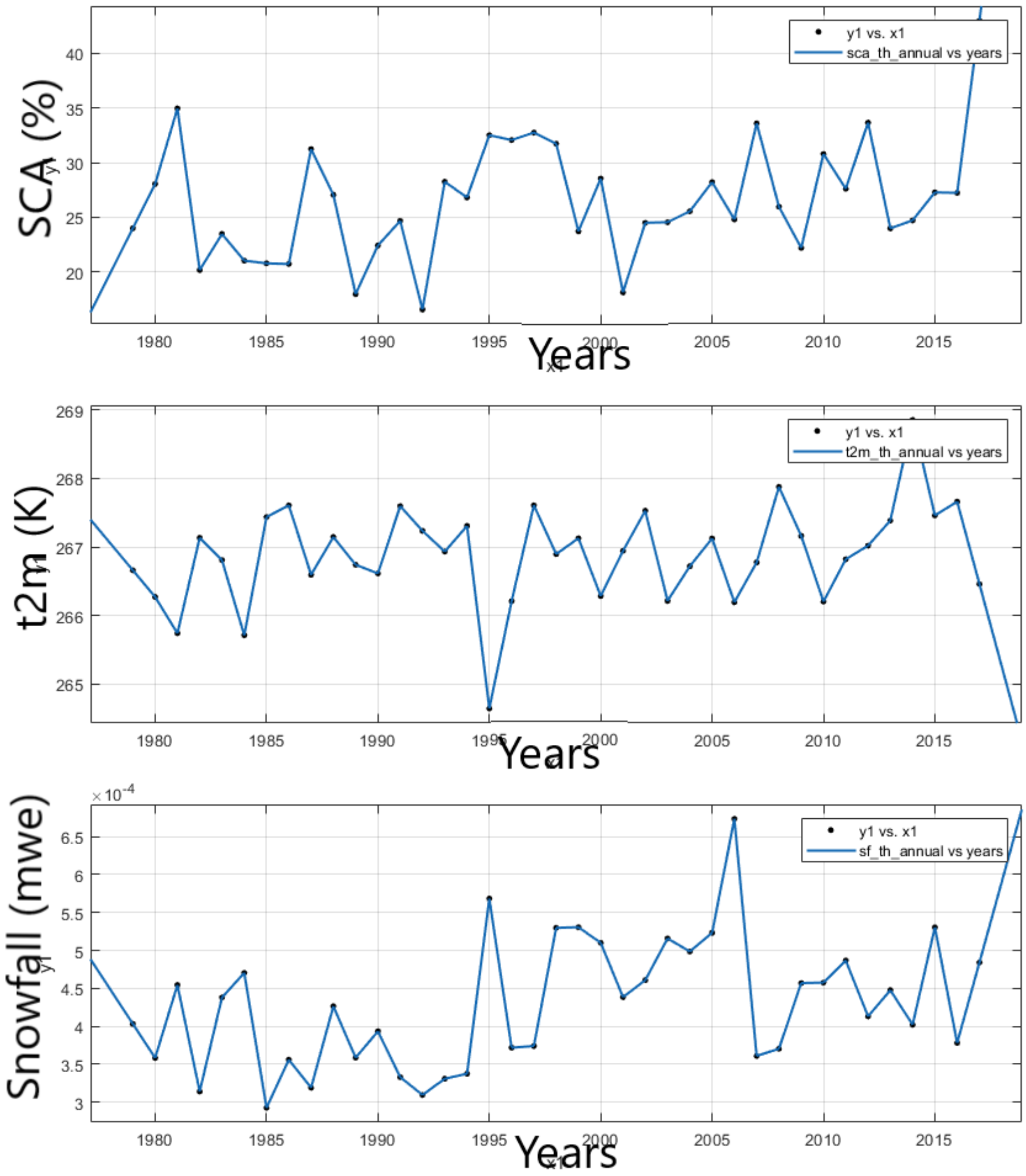

Figure 9 | SCA, Sf & t2m Interpolant Temporal Plots for TH_Annual

DJFM

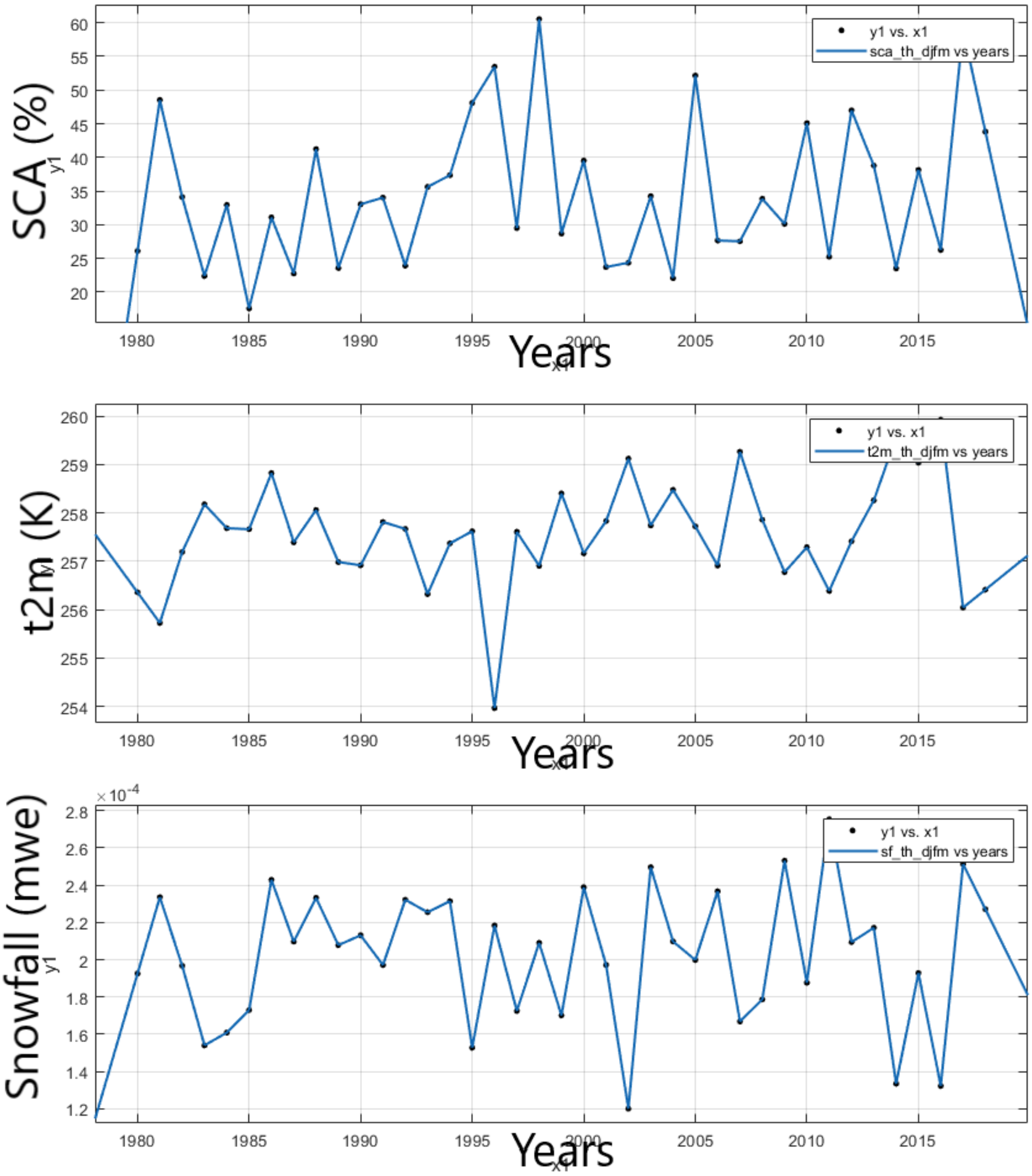

Figure 10 | SCA, Sf & t2m Interpolant Temporal Plots for TH_DJFM

JJAS

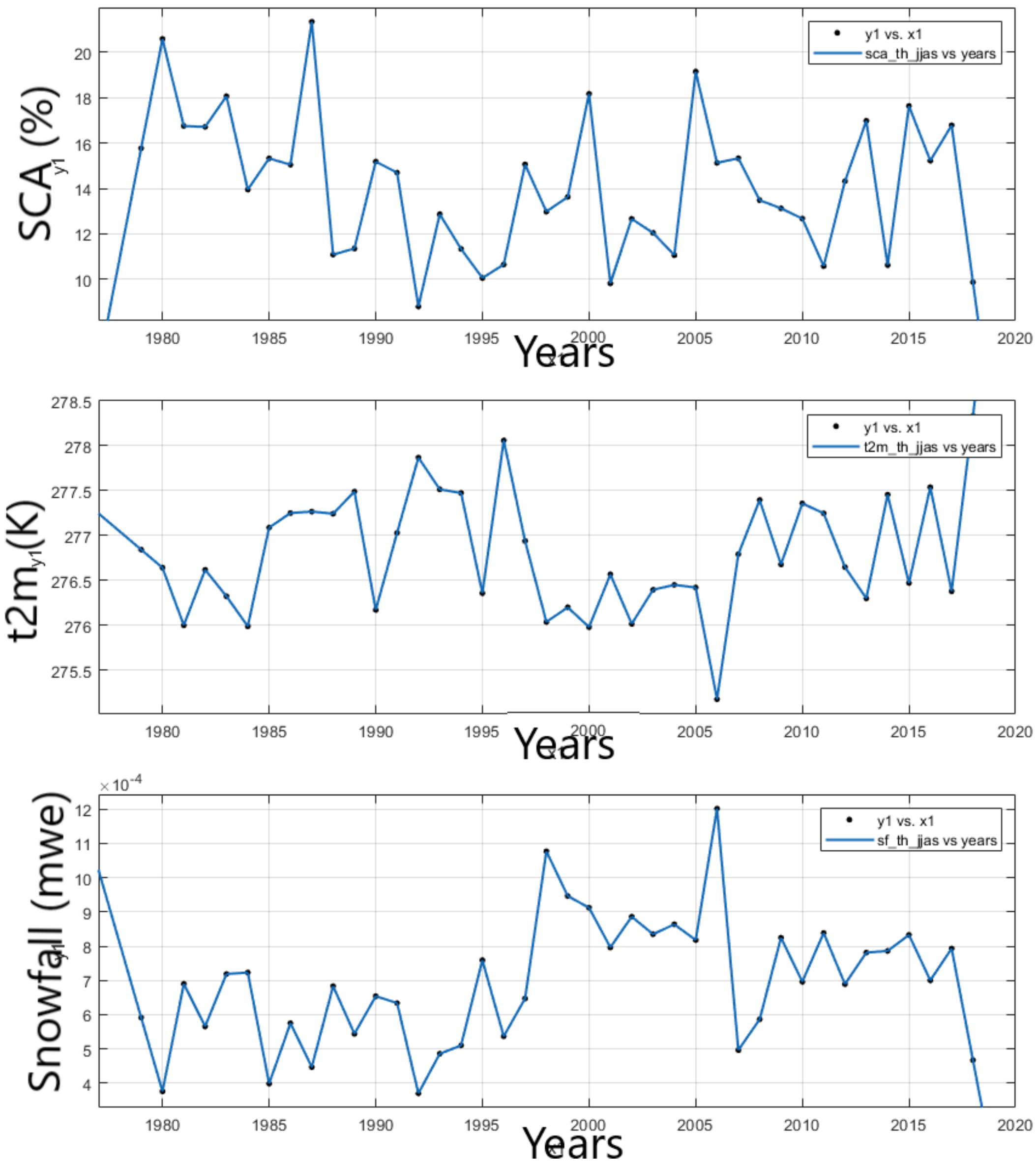

Figure 11 | SCA, Sf & t2m Interpolant Temporal Plots for TH_JJAS

3.1.2. Regressions plots

3.1.2.1. NWH region

3.1.2.1.1. Sf

Annual

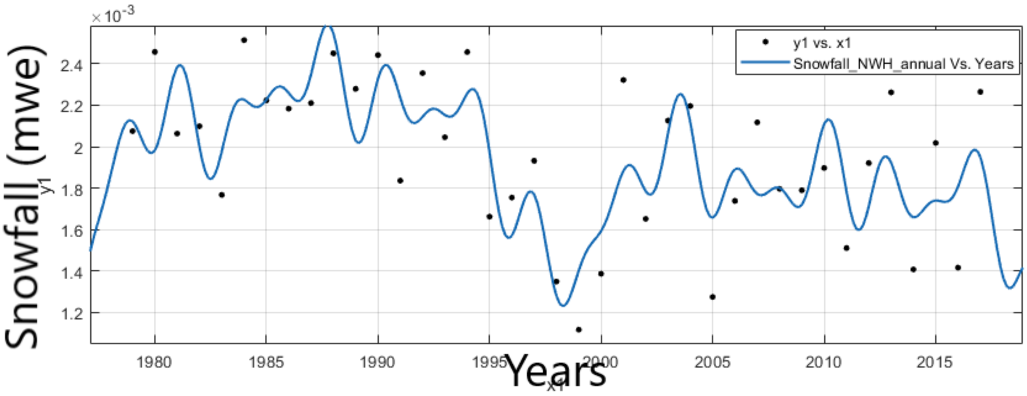

Figure 12 | Sf Temporal Plot for NWH_Annual

Sum of Sines fit, 6 terms

Equation: $f(x) = a_1Sin(b_1x+c_1) + a_2Sin(b_2x+c_1) + a_3Sin(b_3x+c_3) + a_4Sin(b_4x + c_4) + a_4Sin(b_5x + c_5) + a_6Sin(b_6x+c_6)$, where a_1, b_1, c_1 ….. a_6, b_6, c_6 are coefficients.

How good the fit is?:		**Not good fit**	
R^2	Adjusted R^2	RMSE	SSE
0.5627	0.2087	0.000331	2.302e-06

Table 3 | Regression Analysis for Snowfall Vs. Years, NWH_Annual

Winter (DJFM)

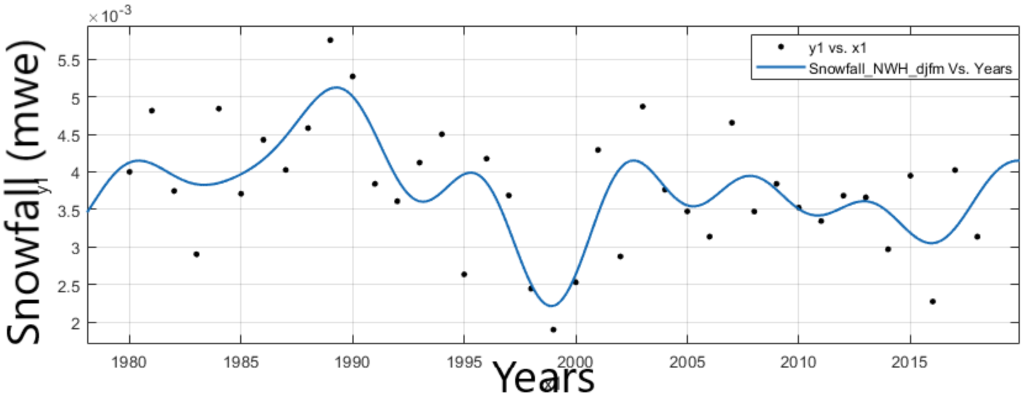

Figure 13 | Sf Temporal Plot for NWH_DJFM

Fourier fit, 7 terms

Equation : $f(x) = a_0 + (a_1Cos(wx) + b_1Sin(wx)) + (a_1Cos(wx) + b_1Sin(wx)) + (a_2Cos(wx) + b_2Sin(wx)) + (a_3Cos(wx) + b_3Sin(wx)) +(a_4Cos(wx) + b_4Sin(wx)) + (a_5Cos(wx) + b_5Sin(wx)) + (a_6Cos(wx) + b_6Sin(wx)) + (a_7Cos(7wx) + b_7Sin(7wx))$, where a_0, b_0, …., a_7, b_7 & w are coefficients.

How good the fit is?:		**Not good fit**	
R^2	Adjusted R^2	RMSE	SSE
0.5106	0.1914	0.000752	1.30×10^{-5}

Table 4 | Regression Analysis for Snowfall Vs. Years, NWH_DJFM

3.1.2.1.2. SCA Annual

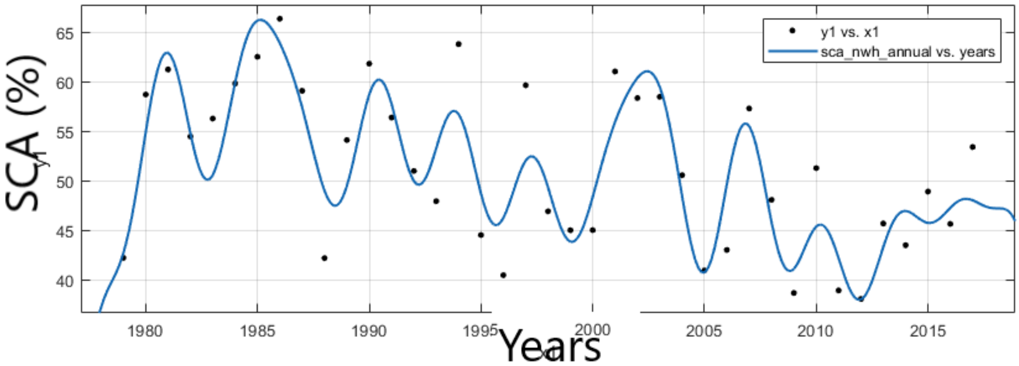

Figure 14 | SCA Temporal Plot for NWH_Annual

Sum of sine fit, 8 terms

Equation: $f(x) = a_1Sin(b_1x+c_1) + a_2Sin(b_2x+c_1) + a_3Sin(b_3x+c_3) + a_4Sin(b_4x + c_4) + a_4Sin(b_5x + c_5) + a_6Sin(b_6x+c_6) + a_7Sin(b_7x+c_7) + a_8Sin(b_8x+c_8)$, where a_1, b_1, c_1 ….. a_8, b_8, c_8 are coefficients.

How good the fit is?:		**Not good fit**	
R^2	Adjusted R^2	RMSE	SSE
0.7794	0.4412	6.087	555.7

Table 5 | Regression Analysis for SCA Vs. Years, NWH_Annual

JJAS

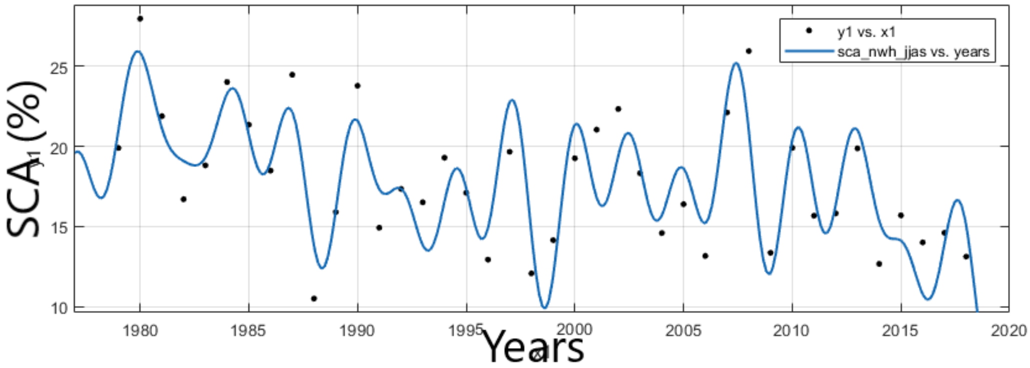

Figure 15 | SCA Temporal Plot for NWH_JJAS

Sum of sines fit, 7 terms

Equation: $f(x) = a_1Sin(b_1x+c_1) + a_2Sin(b_2x+c_1) + a_3Sin(b_3x+c_3) + a_4Sin(b_4x + c_4) + a_4Sin(b_5x + c_5) + a_6Sin(b_6x+c_6) + a_7Sin(b_7x+c_7)$; where a_1, b_1, c_1 ….. a_7, b_7, c_7 are coefficients.

How good the fit is?:		**Not good fit**	
R^2	Adjusted R^2	RMSE	SSE
0.7356	0.4574	3.052	176.9

Table 6 | Regression Analysis for SCA Vs. Years, NWH_JJAS

3.1.2.1.3. t2m

Annual

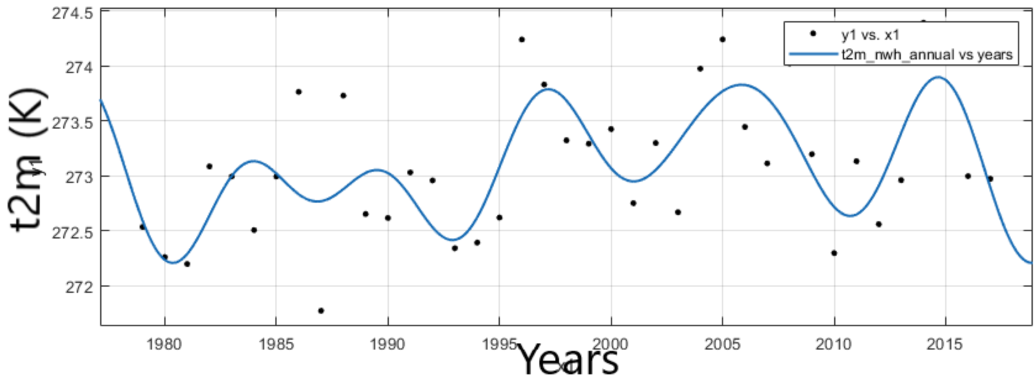

Figure 16 | t2m Temporal Plot for NWH_Annual

Fourier Fit, 6 terms

Equation : $f(x) = a_0 + (a_1Cos(wx) + b_1Sin(wx)) + (a_1Cos(wx) + b_1Sin(wx)) + (a_2Cos(wx) + b_2Sin(wx)) + (a_3Cos(wx) + b_3Sin(wx)) +(a_4Cos(wx) + b_4Sin(wx)) + (a_5Cos(wx) + b_5Sin(wx)) + (a_6Cos(wx) + b_6Sin(wx))$, where a_0, b_0, …., a_6, b_6 & w are coefficients.

How good the fit is?:		Not good fit	
R^2	Adjusted R^2	RMSE	SSE
0.4972	0.2357	0.5634	7.934

Table 7 | Regression Analysis for SCA Vs. Years, NWH_JJAS

3.1.2.2. WH region

3.1.2.2.1. t2m

Annual

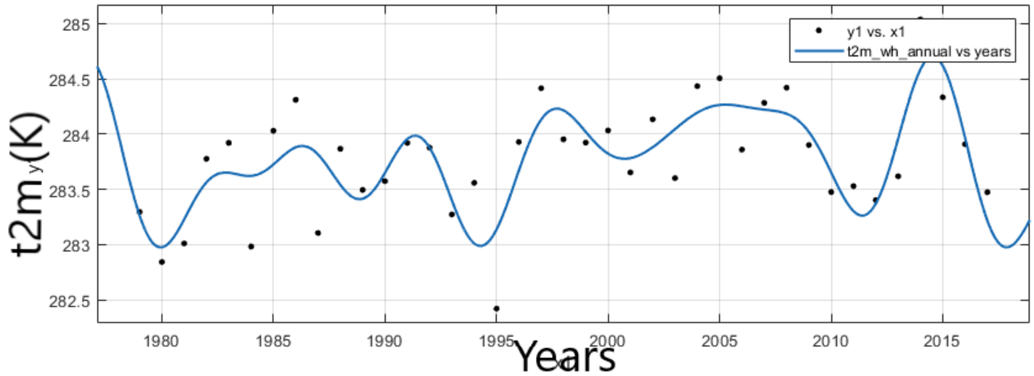

Figure 17 | t2m Temporal Plot for WH_Annual

Fourier Fit, 8 terms

Equation : $f(x) = a_0 + (a_1Cos(wx) + b_1Sin(wx)) + (a_1Cos(wx) + b_1Sin(wx)) + (a_2Cos(wx) + b_2Sin(wx)) + (a_3Cos(wx) + b_3Sin(wx)) + (a_4Cos(wx) + b_4Sin(wx)) + (a_5Cos(wx) + b_5Sin(wx)) + (a_6Cos(wx) + b_6Sin(wx)) + (a_7Cos(7wx) + b_7Sin(7wx)) + (a_8Cos(8wx) + b_8Sin(8wx))$, where a_0, b_0, …., a_8, b_8 & w are coefficients.

How good the fit is?:		Not good fit	
R^2	Adjusted R^2	RMSE	SSE
0.6285	0.3277	0.4233	3.764

Table 8 | Regression Analysis for t2m Vs. Years, WH_Annual

3.1.2.3. TH region

3.1.2.3.1. Sf

Annual

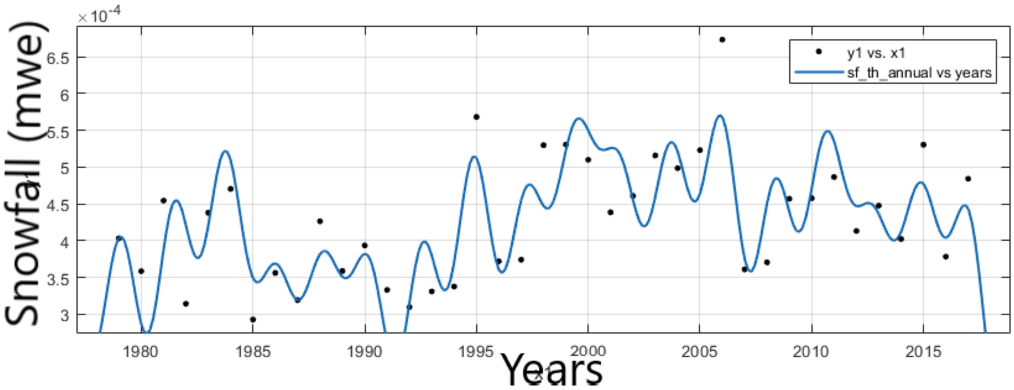

Figure 18 | Sf Temporal Plot for TH_Annual

Sum of Sines fit, 6 terms

Equation: $f(x) = a_1Sin(b_1x+c_1) + a_2Sin(b_2x+c_1) + a_3Sin(b_3x+c_3) + a_4Sin(b_4x + c_4) + a_4Sin(b_5x + c_5) + a_6Sin(b_6x+c_6)$, where a_1, b_1, c_1 ….. a_6, b_6, c_6 are coefficients.

How good the fit is?:		**Not good fit**	
R^2	Adjusted R^2	RMSE	SSE
0.6407	0.3499	6.799e-05	9.708×10^{-8}

Table 9 | Regression Analysis for Sf Vs. Years, TH_Annual

JJAS

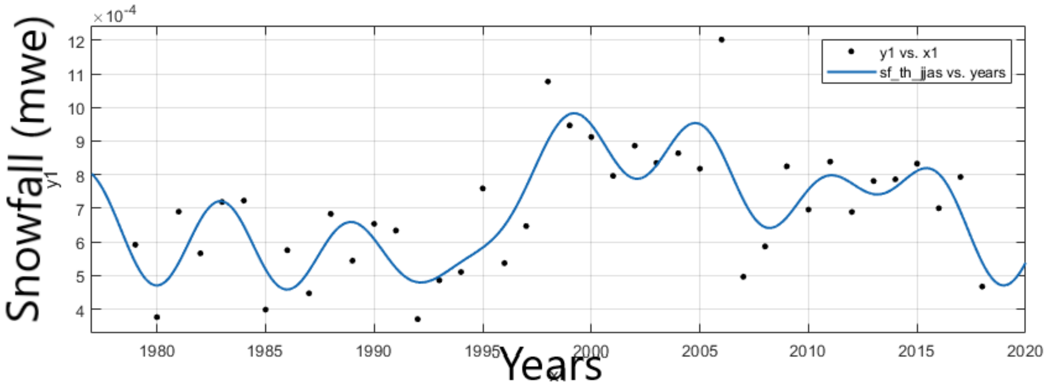

Figure 19 | Sf Temporal Plot for TH_JJAS

Fourier fit, 7 terms

Equation : $f(x) = a_0 + (a_1Cos(wx) + b_1Sin(wx)) + (a_1Cos(wx) + b_1Sin(wx)) + (a_2Cos(wx) + b_2Sin(wx)) + (a_3Cos(wx) + b_3Sin(wx)) +(a_4Cos(wx) + b_4Sin(wx)) + (a_5Cos(wx) + b_5Sin(wx)) + (a_6Cos(wx) + b_6Sin(wx)) + (a_7Cos(7wx) + b_7Sin(7wx))$, where a_0, b_0, …., a_7, b_7 & w are coefficients.

How good the fit is?:		**Not good fit**	
R^2	Adjusted R^2	RMSE	SSE
0.6399	0.4149	0.0001421	$4.84x10^{-8}$

Table 10 | Regression Analysis for Sf Vs. Years, TH_JJAS

3.2. Trend Analysis (Mann Kendall & ITA)

3.2.1. t2m Trend Analysis

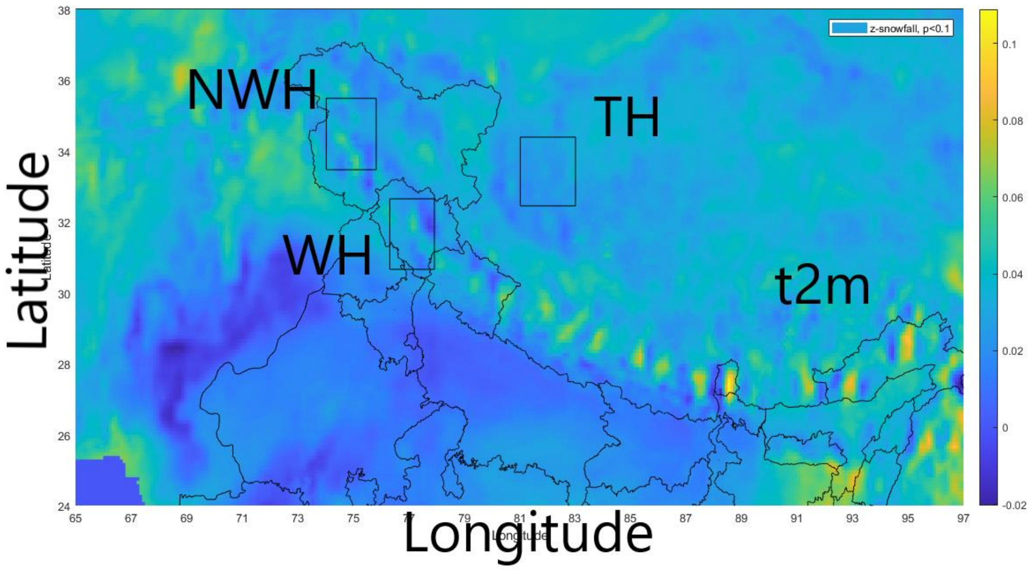

Figure 20 | Kendall Tau Test (Z) for t2m for 40 years of monthly averaged data, square box – 2.1° x 2.1° for 3 locations NWH, WH, TH with 90% confidence.

Himalayas	Temporal Scale	Z (Mann-Kendall)	P- value	Sen's Slope (°C/year)	ITA Slope	Trend
NWH	Annual*	2.30	0.021	0.018	0.023	Increasing
	DJFM	1.21	0.226	0.017	0.020	No Trend
	JJAS	1.32	0.188	0.013	0.006	No Trend
WH	Annual*	2.11	0.035	0.016	0.022	Increasing
	DJFM	1.81	0.070	0.019	0.032	No Trend
	JJAS	1.06	0.290	0.005	0.002	No Trend
TH	Annual	1.52	0.127	0.015	0.017	No Trend
	DJFM	1.08	0.276	0.018	0.040	No Trend
	JJAS	0.66	0.50	0.005	0.011	No Trend

Table 11 | t2m – Mann-Kendall Test, Sen's slope & ITA Slope
Statistically significant* (95%)

Temperature trend analysis for yearly average was carried out at different scales for 3 spatial locations – NWH, WH & TH for the period 1979-2018, the Mann-Kendall, Sen's slope & ITA was determined. Snowfall trend analysis shows that:

- In NWH, only Annual* has significant increasing trend with rate 0.018 °C/year.
- In WH, only Annual* has significant increasing trend with rate 0.016 °C/year.
- In TH, there is no statistically significant trend observed for any temporal scale.

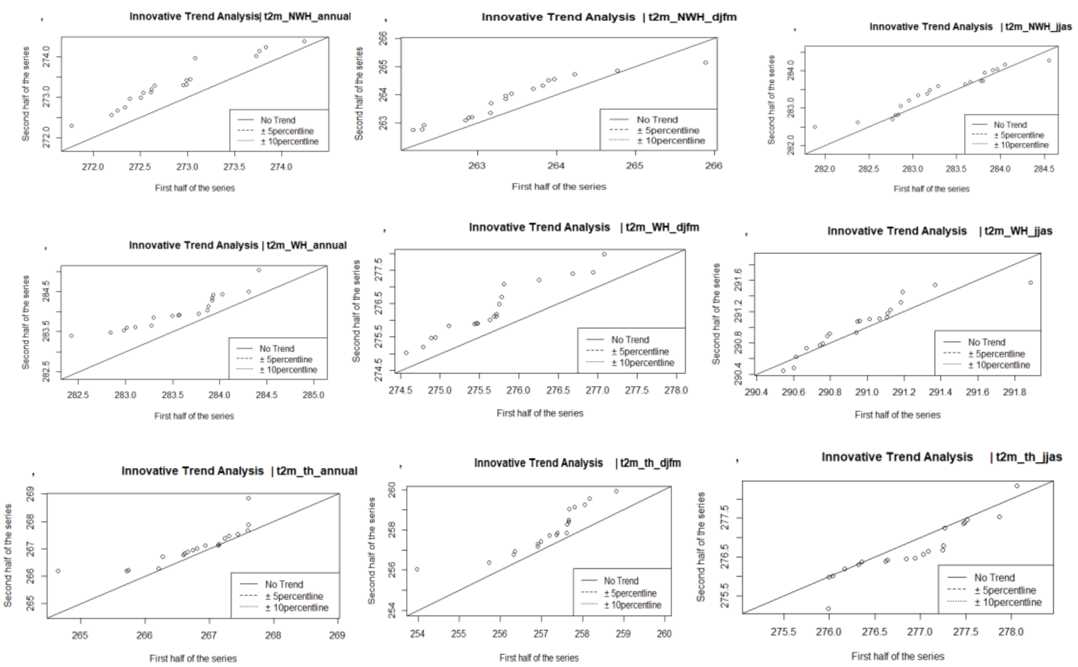

Figure 21 | t2m-ITA for 3 spatial locations in 3 temporal scales of yearly averaged data

Himalayas	Temporal Scale	MK	ITA Low Magnitude	ITA High Magnitude
NWH	Annual*	Yes (+)	Yes (+)	Yes (+)
	DJFM	No	No	No
	JJAS	No	No	No
WH	Annual*	Yes (+)	Yes (+)	Yes (+)
	DJFM	No	Yes (+)	Yes(+)
	JJAS	No	No	No
TH	Annual	No	No	No
	DJFM	No	No	Yes(+)
	JJAS	No	No	No

Table 12 | t2m – MK & ITA Comparison Table

3.2.2. Sf Trend Analysis

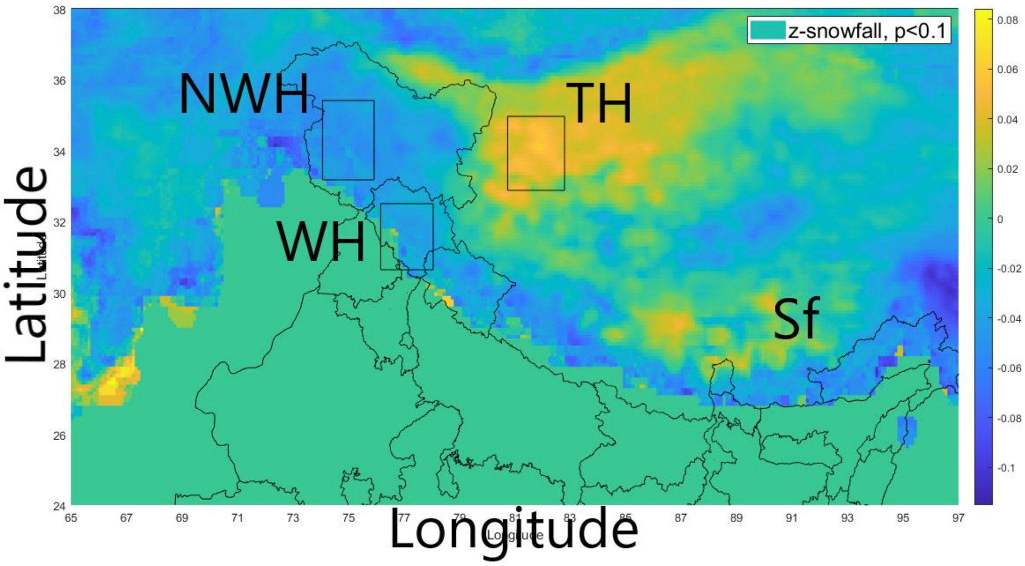

Figure 22 | Kendall Tau Test (Z) for Sf for 40 years of monthly averaged data, square box – 2.1° x 2.1° for 3 locations NWH, WH, TH with 90% confidence.

Himalayas	Temporal Scale	Z (Mann-Kendall)	P- value	Sen's Slope (mm/year)	ITA Slope	Trend
NWH	Annual*	-2.32	0.020	-0.012	-0.000020	Decreasing
	DJFM*	-2.25	0.024	-0.025	-0.000029	Decreasing
	JJAS	-0.87	0.382	-0.002	-0.000002	No Trend
WH	Annual	-1.57	0.113	-0.003	-0.000006	No Trend
	DJFM	-1.38	0.161	-0.007	-0.00001	No Trend
	JJAS	0.99	0.323	0.0009	0.0000008	No Trend
TH	Annual*	2.49	0.012	0.0026	0.0000047	Increasing
	DJFM	0.36	0.711	0.0002	0	No Trend
	JJAS*	2.38	0.016	0.0058	0.0000094	Increasing

Table 11 | Sf – Mann-Kendall Test, Sen's slope & ITA Slope
Statistically significant* (95%)

Snowfall trend analysis for yearly average was carried out at different scales for 3 spatial locations – NWH, WH & TH for the period 1979-2018, the Mann-Kendall, Sen's slope & ITA was determined. Snowfall trend analysis shows that:

- in NWH, Annual* & DJFM* has significant decreasing rate with 0.012 mm/year & 0.025 mm/year respectively.
- In WH, there is no statistically significant trend observed for any temporal scale.
- In TH, Annual* & JJAS* shows significant increasing trends with 2.6×10^{-3} mm/ year & 5.8×10^{-3} mm/year respectively.

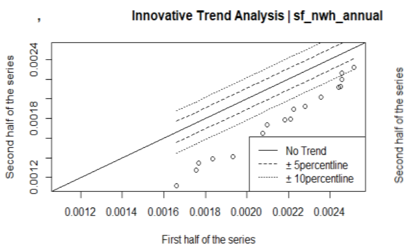

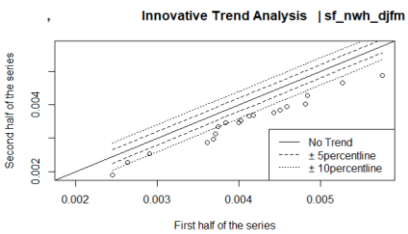

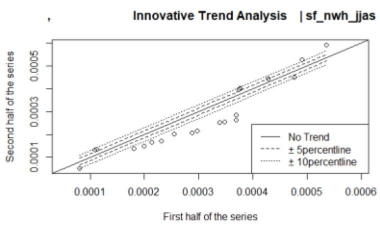

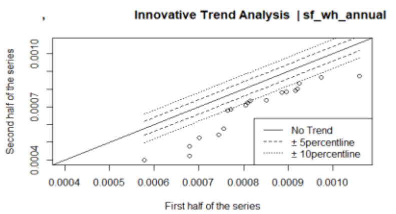

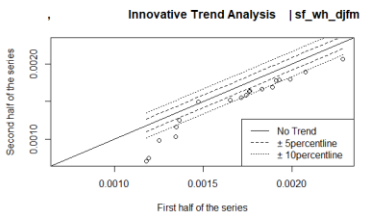

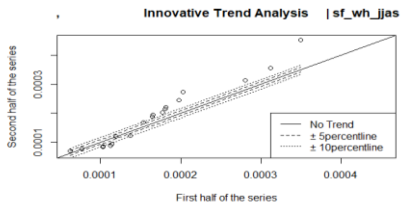

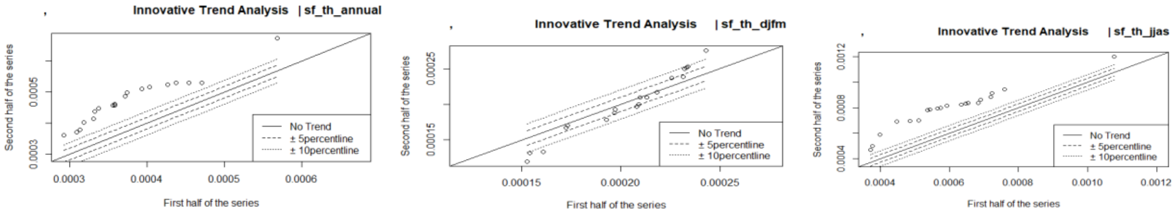

Figure 23 | Sf-ITA for 3 spatial locations in 3 temporal scales of yearly averaged data

Himalayas	**Temporal Scale**	**MK**	**ITA Low Magnitude**	**ITA High Magnitude**
NWH	Annual*	Yes (-)	Yes (-)	Yes (-)
	DJFM*	Yes (-)	Yes (-)	Yes (-)
	JJAS	No	Yes (-)	No
WH	Annual	No	Yes (-)	Yes (-)
	DJFM	No	Yes (-)	No
	JJAS	No	No	Yes (+)
TH	Annual*	Yes (+)	Yes (+)	No
	DJFM	No	Yes (-)	No
	JJAS*	Yes (+)	Yes (+)	No

Table 14 | Sf – MK & ITA Comparison Table

Here, it can be observed from ITA analysis, low magnitude snowfall values have increasing & decreasing trends in TH but high magnitude snowfall value have no trend for all 3 temporal scales.

3.2.3. SCA Trend Analysis

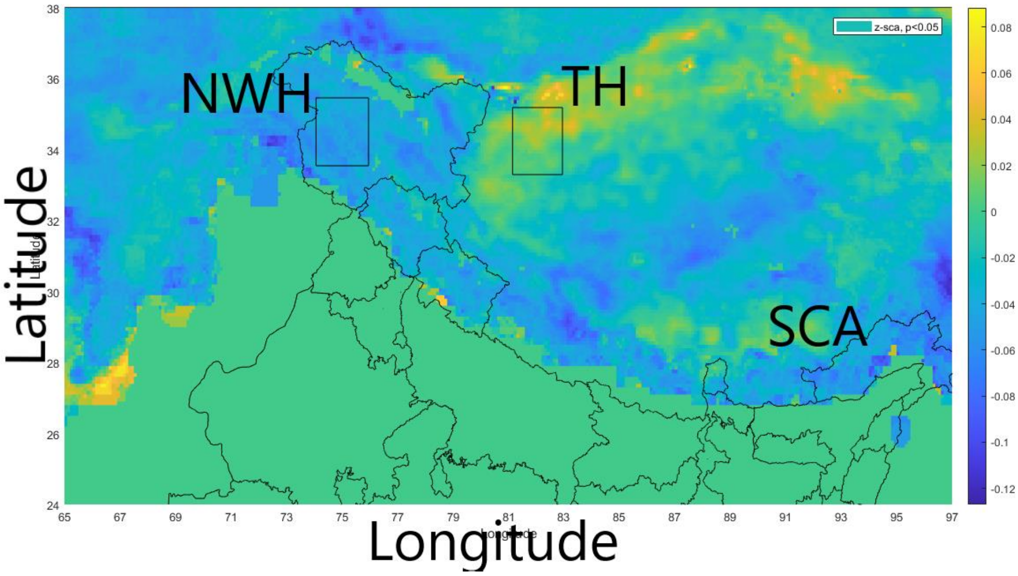

Figure 24 | Kendall Tau Test (Z) for SCA for 40 years of monthly averaged data, square box – 2.1° x 2.1° for 3 locations NWH, WH, TH with 95% confidence.

Himalayas	Temporal Scale	Z (Mann-Kendall)	P -value	Sen's Slope (%/year)	ITA Slope	Trend
NWH	Annual*	-2.80	0.005	-0.35	-0.37	Decreasing
	DJFM	-1.88	0.059	-0.34	-0.37	No Trend
	JJAS*	-2.52	0.011	-0.13	-0.07	Decreasing
TH	Annual	1.84	0.069	0.14	0.06	No Trend
	DJFM	1.23	0.217	0.17	-0.02	No Trend
	JJAS	-1.31	0.188	-0.059	-0.02	No Trend

Table 15 | SCA – Mann-Kendall Test, Sen's slope & ITA Slope
Statistically significant* (95%)

SCA trend analysis for yearly average was carried out at different scales for 3 spatial locations –NWH, WH & TH for the period 1979-2018, the Mann-Kendall, Sen's slope & ITA slope was determined. SCA trend analysis shows that:

- In NWH, Annual* & JJAS* has significant decreasing rate with 0.35 %/year & 0.13 %/year respectively.
- In WH, there is no statistically significant trend square box captured.
- In TH, there is no statistically significant trend observed for any temporal scale.

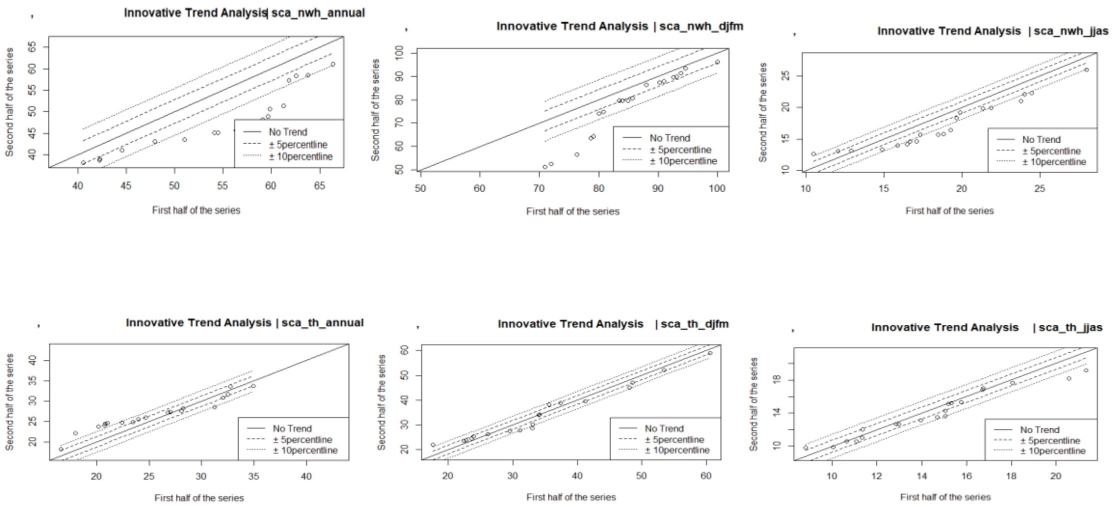

Figure 25 | SCA-ITA for 3 spatial locations in 3 temporal scales of yearly averaged data

Himalayas	**Temporal Scale**	**MK**	**ITA Low Magnitude**	**ITA High Magnitude**
NWH	Annual*	Yes (-)	No	Yes (-)
	DJFM	No	Yes (-)	No
	JJAS*	Yes (-)	No	Yes (-)
TH	Annual	No	Yes (+)	No
	DJFM	No	No	No
	JJAS	No	Yes (+)	No

Table 16 | SCA – MK & ITA Comparison Table

3.2.4. SDE Trend Analysis

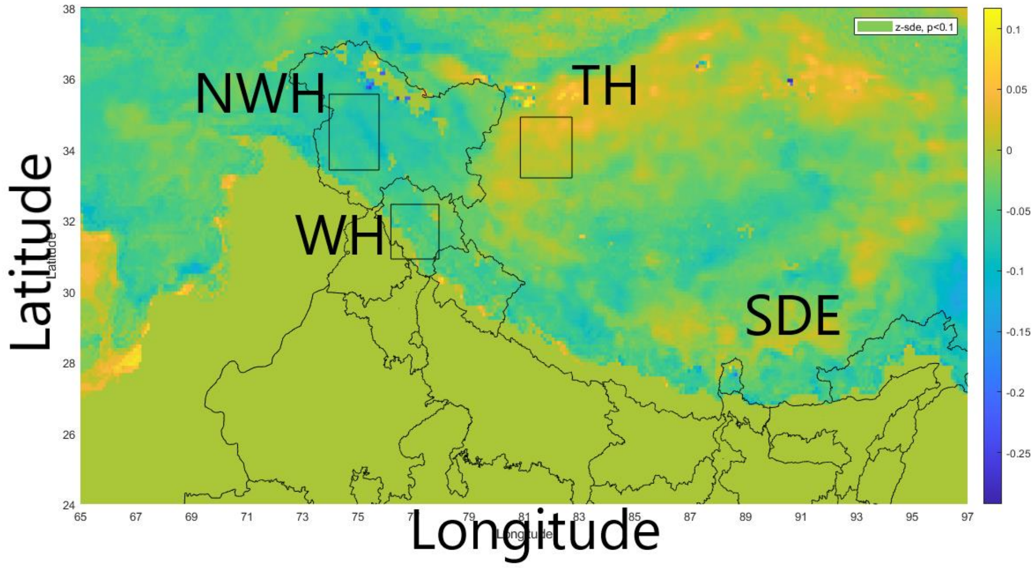

Figure 26 | Kendall Tau Test (Z) for SDE for 40 years of monthly averaged data, square box – 2.1° x 2.1° for 3 locations NWH, WH, TH with 90% confidence.

Himalayas	Temporal Scale	Z (Mann-Kendall)	P-value	Sen's Slope (m/year)	ITA Slope	Trend
NWH	Annual*	-2.90	0.004	-0.007	-0.010	Decreasing
	DJFM*	-2.25	0.024	-0.008	-0.011	Decreasing
	JJAS*	-2.36	0.018	-0.004	-0.005	Decreasing
WH	Annual	-1.88	0.059	-0.003	-0.004	No Trend
	DJFM	-1.25	0.208	-0.002	-0.003	No Trend
	JJAS	-1.76	0.078	-0.002	-0.002	No Trend
TH	Annual	-0.19	0.846	-0.000	-0.000	No Trend
	DJFM	0.41	0.681	0.000	0.000	No Trend
	JJAS*	+2.29	0.022	+0.01	+0.01	Increasing

Table 17 | SDE – Mann-Kendall Test, Sen's slope & ITA Slope
Statistically significant* (95%)

SDE trend analysis for yearly average was carried out at different scales for 3 spatial locations –NWH, WH & TH for the period 1979-2018, the Mann-Kendall, Sen's slope & ITA slope was determined. SDE trend analysis shows that:

- In NWH, Annual*, DJFM* & JJAS* (all scales) has significant decreasing rates with 0.07 m/year, 0.008 m/year & 0.004 m/year respectively.
- In WH, there is no statistically significant trends observed for any temporal scale.

- In TH, only JJAS* scale shows significant magnitude increasing trend.

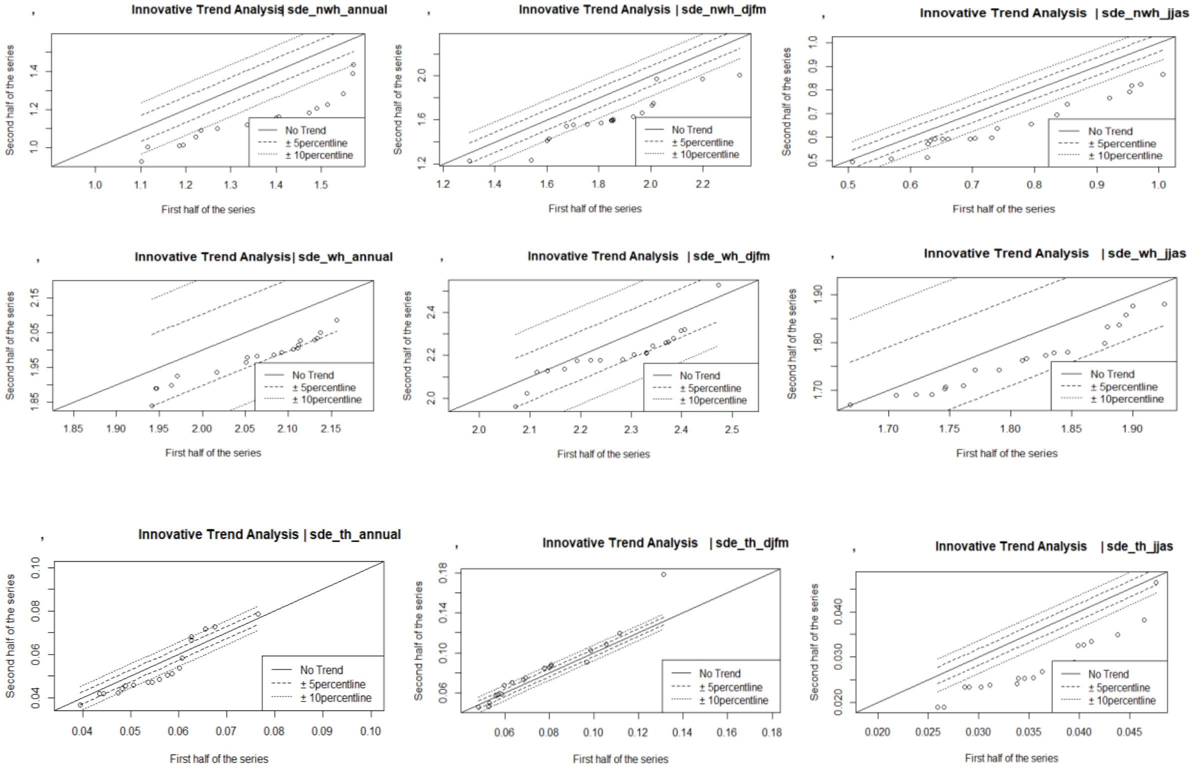

Figure 27 | SDE-ITA for 3 spatial locations in 3 temporal scales of yearly averaged data

Himalayas	Temporal Scale	MK	ITA Low Magnitude	ITA High Magnitude
NWH	Annual*	Yes (-)	Yes (-)	Yes (-)
	DJFM*	Yes (-)	No	Yes (-)
	JJAS*	Yes (-)	Yes (-)	Yes (-)
WH	Annual	No	No	No
	DJFM	No	No	No
	JJAS	No	No	No
TH	Annual	No	No	No
	DJFM	No	No	No
	JJAS*	Yes (+)	Yes (+)	Yes (+)

Table 18 | SDE – MK & ITA Comparison Table

3.2.5. STR Trend Analysis

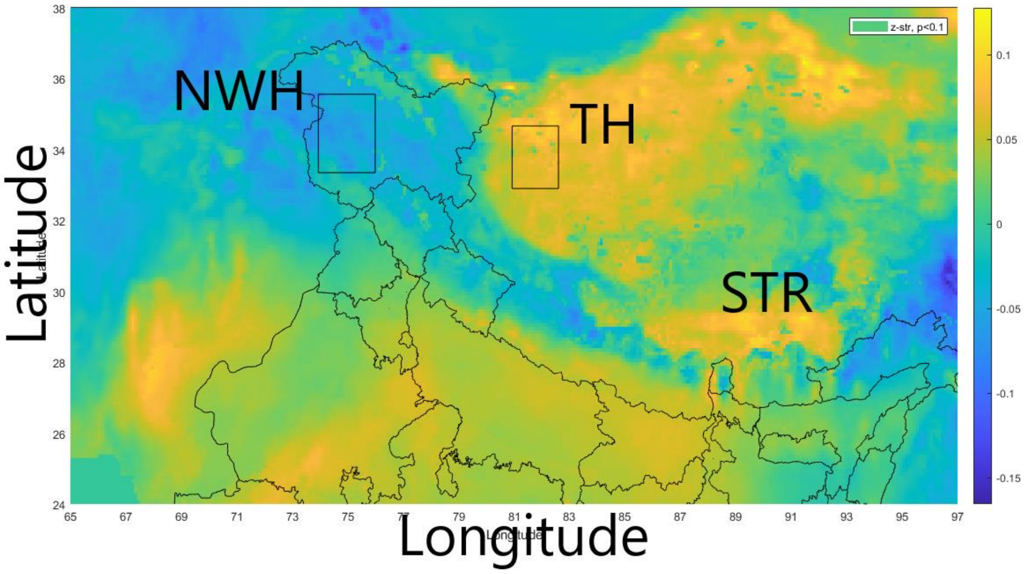

Figure 28 | Kendall Tau Test (Z) for STR for 40 years of monthly averaged data, square box – 2.1° x 2.1° for 3 locations NWH, WH, TH with 90% confidence.

Himalayas	Temporal Scale	Z (Mann-Kendall)	P - value	Sen's Slope (J/m^2 year)	ITA Slope	Trend
NWH	Annual	-1.79	0.073	-9934.85	-12699.10	No Trend
	DJFM	-1.69	0.090	-11838.5	-13284.88	No Trend
	JJAS	-0.85	0.395	-5331.44	-1748.97	No Trend
TH	Annual*	2.58	0.009	14273	20901.60	Increasing
	DJFM	-0.79	0.424	-4201.26	-8271.51	No Trend
	JJAS*	2.94	0.003	33607.75	45871.04	Increasing

Table 19 | STR - Mann_Kendall Test, Sen's slope & ITA Slope statistically significant* (95%)

STR trend analysis for yearly average was carried out at different scales for 3 spatial locations –NWH, WH & TH for the period 1979-2018, the Mann-Kendall, Sen's slope & ITA slope was determined. STR trend analysis shows that:

- In NWH, there is no statistically significant trends observed for any temporal scale.
- In WH, there is no statistically significant trend square box captured.
- In TH, Annual* & JJAS* scale shows significant increasing trend with rates 20901.60 J/m^2 year & 45871.04 J/m^2 year respectively.

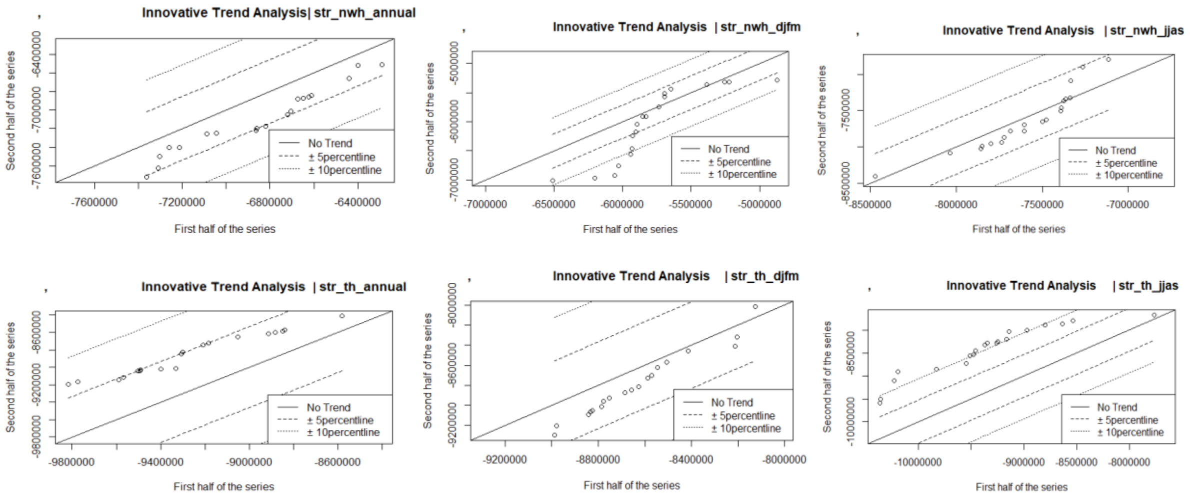

Figure 29 | STR-ITA for 3 spatial locations in 3 temporal scales of yearly averaged data

Himalayas	**Temporal Scale**	**MK**	**ITA Low Magnitude**	**ITA High Magnitude**
NWH	Annual	No	No	No
	DJFM	No	No	No
	JJAS	No	No	No
TH	Annual*	Yes (+)	No	No
	DJFM	No	No	No
	JJAS*	Yes (+)	Yes (+)	No

Table 20 | STR – MK & ITA Comparison Table

3.2.6. SSHF Trend Analysis

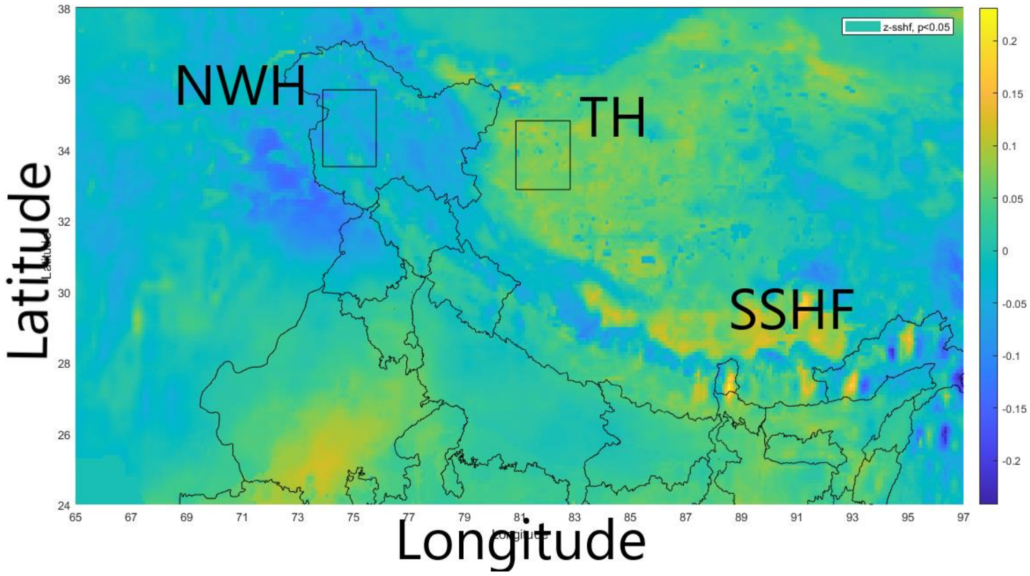

Figure 30 | Kendall Tau Test (Z) for SSHF for 40 years of monthly averaged data, square box – 2.1° x 2.1° for 3 locations NWH, WH, TH with 95% confidence.

Himalayas	Temporal Scale	Z (Mann-Kendall)	P -value	Sen's Slope (J/m^2 year)	ITA Slope	Trend
NWH	Annual*	-2.51	0.011	-7722.87	-9328.44	Decreasing
	DJFM	-1.71	0.085	-3794.86	-6059.16	No Trend
	JJAS	-1.52	0.127	-4929.21	-3711.25	No Trend
TH	Annual*	3.07	0.002	14428.95	21594.59	Increasing
	DJFM	0.56	0.578	1265.39	3515.74	No Trend
	JJAS*	3.22	0.001	25868.83	37588.44	Increasing

Table 21 | SSHF - Mann_Kendall Test, Sen's slope & ITA Slope
Statistically significant* (95%)

SSHF trend analysis for yearly average was carried out at different scales for 3 spatial locations –NWH, WH & TH for the period 1979-2018, the Mann-Kendall, Sen's slope & ITA slope was determined. SSHF trend analysis shows that:

- In NWH, only Annual* scale shows significant decreasing trends with rate 7722.87 J/m^2 year.
- In WH, there is no statistically significant trend square box captured.
- In TH, Annual* & JJAS* scale shows significant increasing trend with rates 14428.95 J/m^2 year & 25868.83 J/m^2 year respectively.

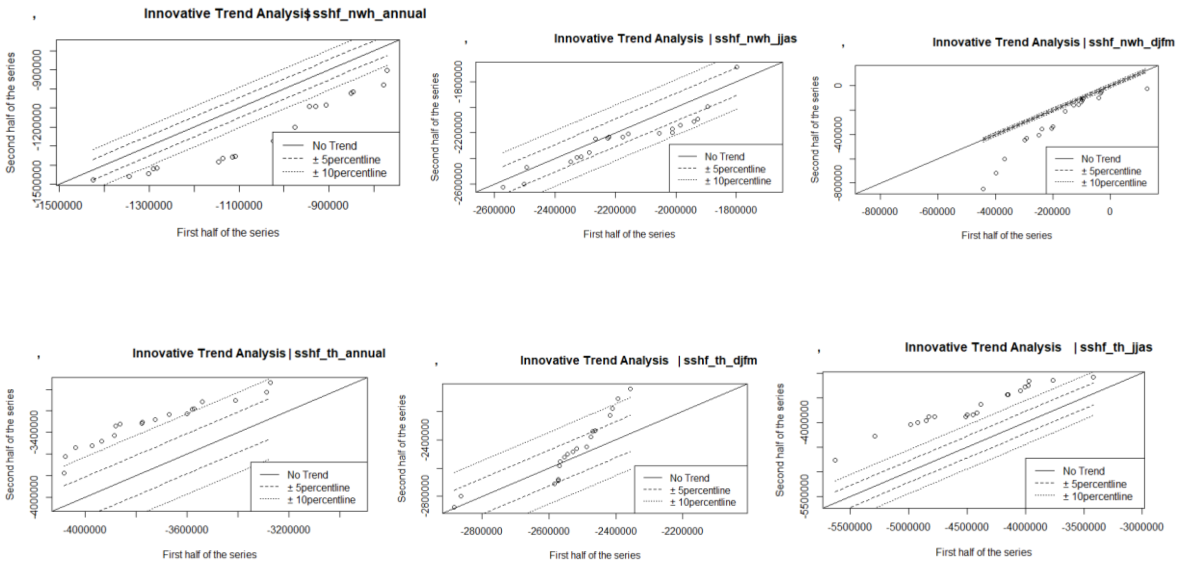

Figure 31| SSHF-ITA for 3 spatial locations in 3 temporal scales of yearly averaged data

Himalayas	Temporal Scale	MK	ITA Low Magnitude	ITA High Magnitude
NWH	Annual*	Yes (-)	Yes (-)	Yes (-)
	DJFM	No	No	No
	JJAS	No	Yes (-)	Yes (-)
TH	Annual*	Yes (+)	Yes (+)	No
	DJFM	No	No	No
	JJAS*	Yes (+)	Yes (+)	Yes (+)

Table 22 | SSHF – MK & ITA Comparison Table

3.3. Snowfall of Study Areas

Himalayas Sf Mean (mwe)	NWH	WH	TH
Annual	0.0012	0.007	0.00040
DJFM	0.0030	0.0010	0.0002
JJAS	0.0001	0.0007	0.00017

Table 23 | Analyzing Mean DJFM (Winter) Sf of all 3 Study Areas (40 Years)

3.4. Comparison of SCA trends among Study Areas

Himalayas SCA trends	NWH	WH	TH
Annual	Decreasing*	Nil	No Trend
DJFM	No Trend	Nil	No Trend
JJAS	Decreasing*	Nil	No Trend
Statistically significant*			

Table 24 | Comparison of SCA trends among regions of Study Area (40 Years)

3.5. Correlation Analysis

3.5.1. Association of SCA with Climate Variables

The strength of SCA's association with snowfall & temperature was determined using Spearman's Correlation method [28] at NWH, WH & TH locations. The analysis showed statistically significant strong negative correlation between SCA & annual t2m with correlation coefficient ranging between -0.77 to -0.82 over the past 40 years for all 3 Himalayan locations. Similar results were observed in Yadav & Choudhary [28] for NWH region. It shows that increase or decrease in temperature implies a decrease or increase in SCA respectively for all 3 locations for almost all temporal scales calculated. These results proves that decreasing SCA coincides with increasing t2m and decreased sf values over all 3 regions for almost all 3 temporal scales illustrated by *3.1.1. Interpolant plots* & *3.1.2. Regression plots*. For instance, in interpolant plots for NWH region for SCA, t2m and snowfall respectively for annual scale here we can see for year 1995, SCA is decreasing, at the same time period, t2m is increasing and snowfall is decreasing as well.

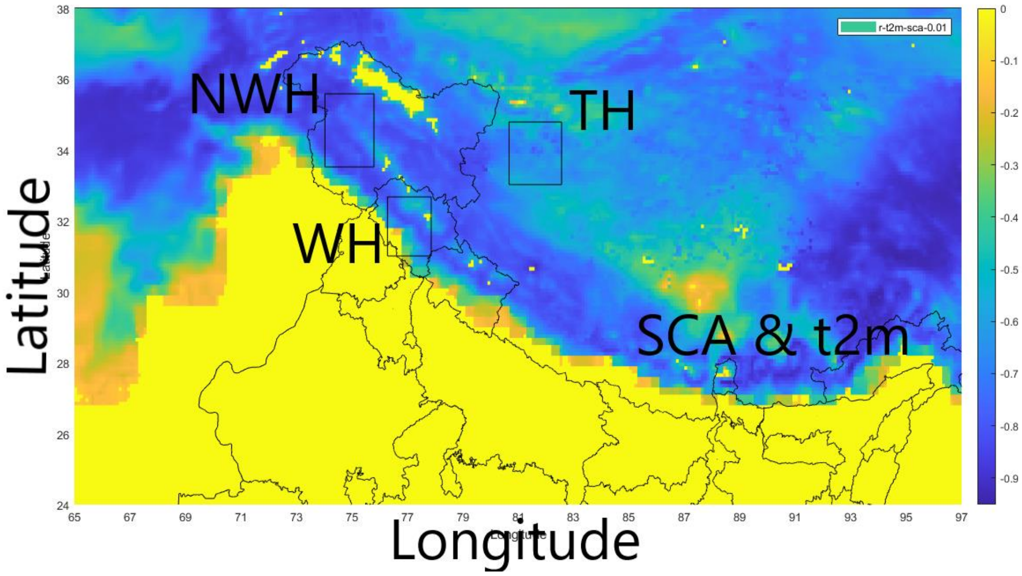

Figure 32 | Correlation (r) for SCA and Sf for 40 years of monthly averaged data, square box – 2.1° x 2.1° with 99% confidence.

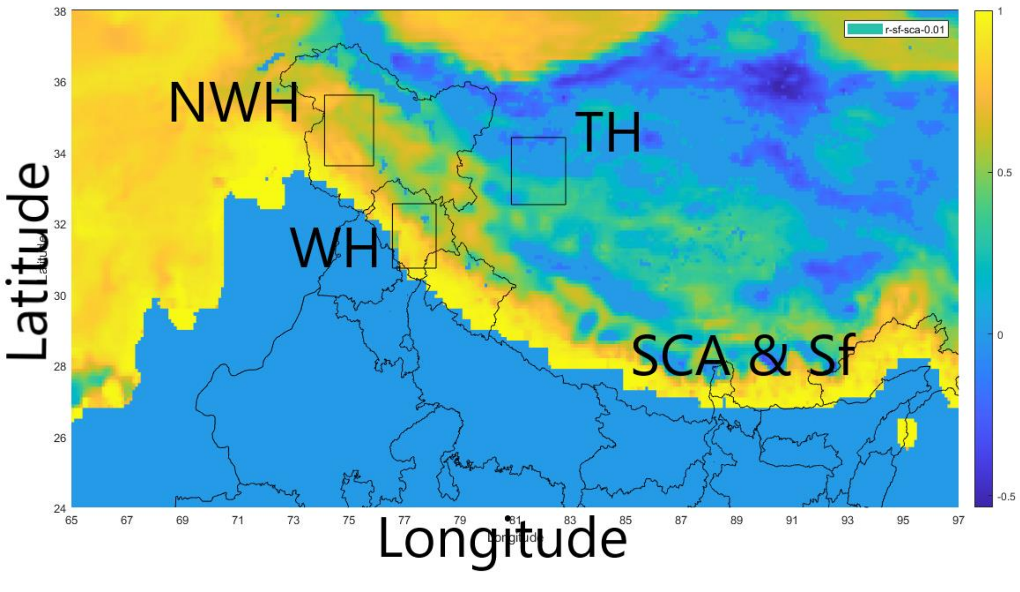

Figure 33 |Correlation (r) for t2m and SCA for 40 years of monthly averaged data, square box – 2.1° x 2.1° with 99% confidence.

3.5.1.1. NWH

SCA/Temporal Scale -NWH	Annual	DJFM	JJAS
T2m	-0.81* $p=2.5 \times 10^{-8}$	-0.33* $P = 0.036$	-0.73* $p = 4.1 \times 10^{-7}$
Sf	0.78* $P = 2.1 \times 10^{-9}$	0.19 $P = 0.22$	0.61* $P = 3.2 \times 10^{-5}$

Table 25 | Spearman Correlation of SCA with Sf & t2m for NWH
***statistically significant**

In NWH region, SCA and t2m are strongly correlated during the annual & monsoon (JJAS) period but very weakly during Winter (DJFM) period. During the monsoon period, SCA is strongly correlated with both t2m and snowfall but in winter period, SCA is weakly correlated with t2m and in contrast a non-significant correlation exists between sf and SCA, which suggests that temperature slightly dominates over snowfall for controlling SCA even during winter period.

3.5.1.1.1. Correlation Plots:

3.5.1.1.1.1. SCA vs. t2m Annual

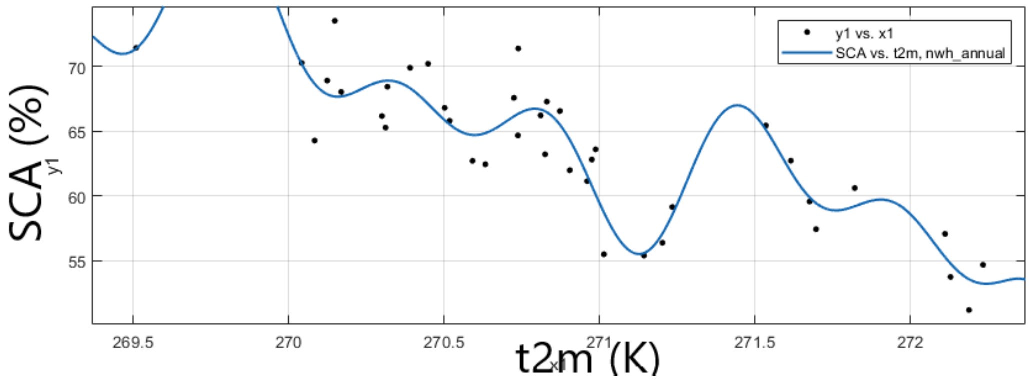

Figure 34 | SCA vs. t2m, NWH_Annual

Sum of Sines fit, 6 terms

Equation: $f(x) = a_1\text{Sin}(b_1x+c_1) + a_2\text{Sin}(b_2x+c_1) + a_3\text{Sin}(b_3x+c_3) + a_4\text{Sin}(b_4x + c_4) + a_4\text{Sin}(b_5x + c_5) + a_6\text{Sin}(b_6x+c_6)$, where $a_1, b_1, c_1 \ldots\ldots a_6, b_6, c_6$ are coefficients.

How good the fit is?:		Not good fit	
R^2	Adjusted R^2	RMSE	SSE
0.8313	0.7625	2.681	194

Table 26 | Regression Analysis for SCA Vs. t2m, NWH_Annual

DJFM

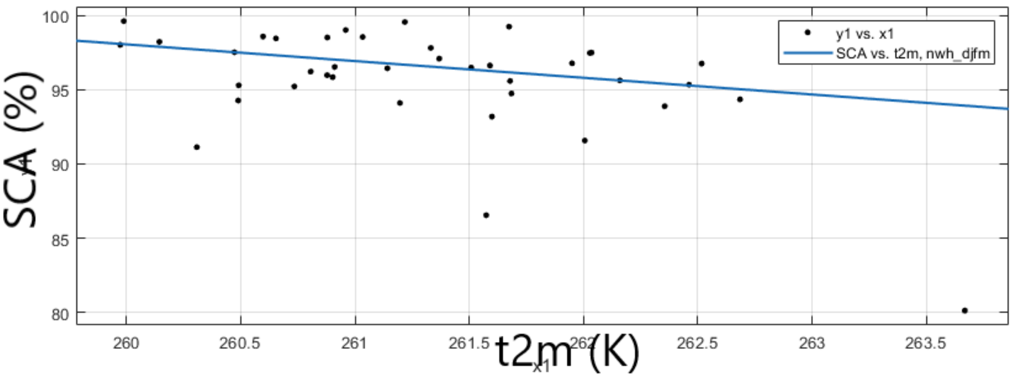

Figure 35 | SCA vs. t2m, NWH_DJFM

Linear Fit, 2 coefficients, Robust = LAR,

$f(x) = p_1x + p_2$, where p_1 & p_2 are coefficients, $p_1 = -0.914$ & $p_2 = 96.57$

How good the fit is?:		**Not good fit**	
R^2	Adjusted R^2	RMSE	SSE
0.6558	0.6465	2.158	172.2

Table 27 | Regression Analysis for SCA Vs. t2m, NWH_DJFM

JJAS

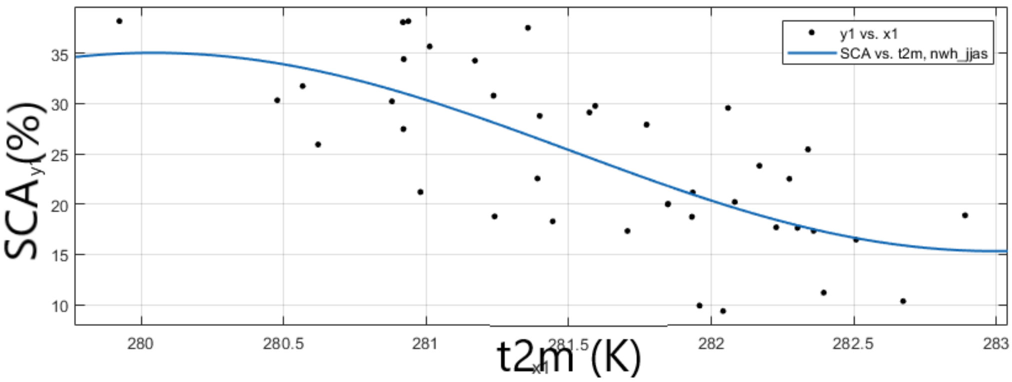

Figure 36 | SCA vs. t2m, NWH_JJAS

Fourier Fit, 1 term

Equation: $f(x) = a_0 + a_1Cos(wx) + b_1Sin(wx)$, where a_0, a_1, b_1 and 'w' are coefficients.

How good the fit is?:		Not good fit	
R^2	Adjusted R^2	RMSE	SSE
0.5137	0.4732	5.957	1

Table 28 | Regression Analysis for SCA Vs. t2m, NWH_JJAS

3.5.1.1.1.2. SCA vs Sf

Annual

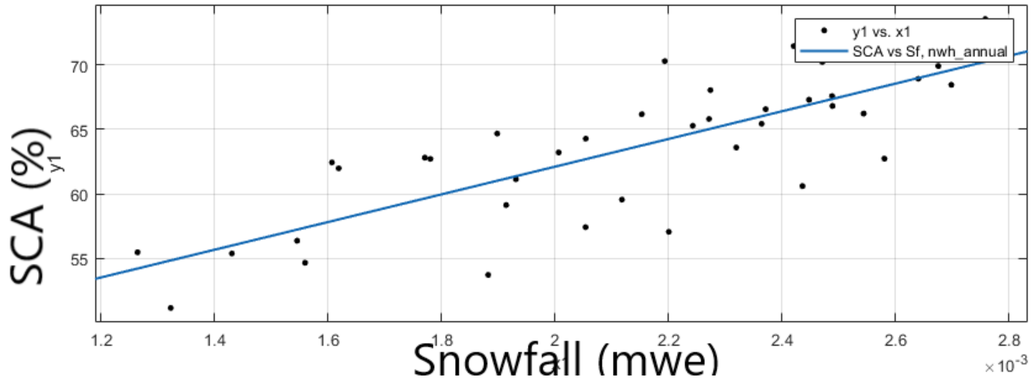

Figure 37 | SCA vs. Sf, NWH_Annual

Linear Fit, 2 coefficients

$f(x) = p_1x + p_2$, where p_1 & p_2 are coefficients, $p_1 = 1.07 \times 10^4$ & $p_2 = 40.69$

How good the fit is?:		Not good fit	
R^2	Adjusted R^2	RMSE	SSE
0.6247	0.6146	3.415	431.5

Table 29 | Regression Analysis for SCA Vs. Sf, NWH_Annual

JJAS

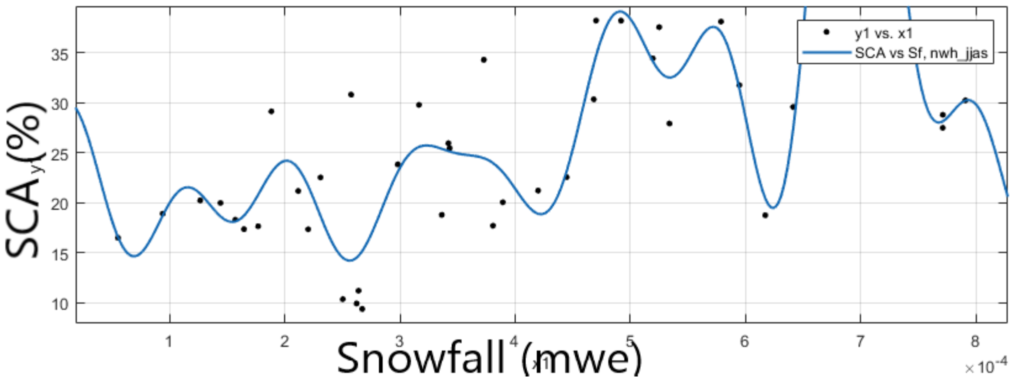

Figure 38 | SCA vs. Sf, NWH_JJAS

Fourier 8 terms

Equation : $f(x) = a_0 + (a_1Cos(wx) + b_1Sin(wx)) + (a_1Cos(wx) + b_1Sin(wx)) + (a_2Cos(wx) + b_2Sin(wx)) + (a_3Cos(wx) + b_3Sin(wx)) + (a_4Cos(wx) + b_4Sin(wx)) + (a_5Cos(wx) + b_5Sin(wx)) + (a_6Cos(wx) + b_6Sin(wx)) + (a_7Cos(7wx) + b_7Sin(7wx)) + (a_8Cos(8wx) + b_8Sin(8wx))$, where, a_0, b_0, …., a_8, b_8 & w are coefficients.

How good the fit is?:		**Not good fit**	
R^2	Adjusted R^2	RMSE	SSE
0.7187	0.5013	5.796	739

Table 30 | Regression Analysis for SCA Vs. Sf, NWH_JJAS

3.5.1.2. WH

SCA With WH	**Annual**	**DJFM**	**JJAS**
T2m	-0.82* $P = 1.2 \times 10^{-8}$	-0.74* $P = 3.4 \times 10^{-7}$	-0.63* $P = 2 \times 10^{-5}$
Sf	0.56* $P = 2.5 \times 10^{-4}$	0.57* $P = 1.8 \times 10^{-4}$	0.23 $P = 0.13$

***statistically significant**

Table 31 | Spearman Correlation of SCA with Sf & t2m for WH

In WH region, SCA and t2m are strongly correlated during the annual period & moderately during JJAS & DJFM periods. During the monsoon period, a strong correlation exists between SCA & t2m and in contrast weak non-significant correlation exists between SCA & Sf suggesting that for controlling SCA, t2m dominates over snowfall. But in winter & annual period, SCA is controlled by both t2m and sf with t2m on the higher side since strong correlations exists between SCA & t2m and moderate correlations exists between sf and SCA.

3.5.1.2.1. Correlation Plots

3.5.1.2.1.1. SCA vs t2m

Annual

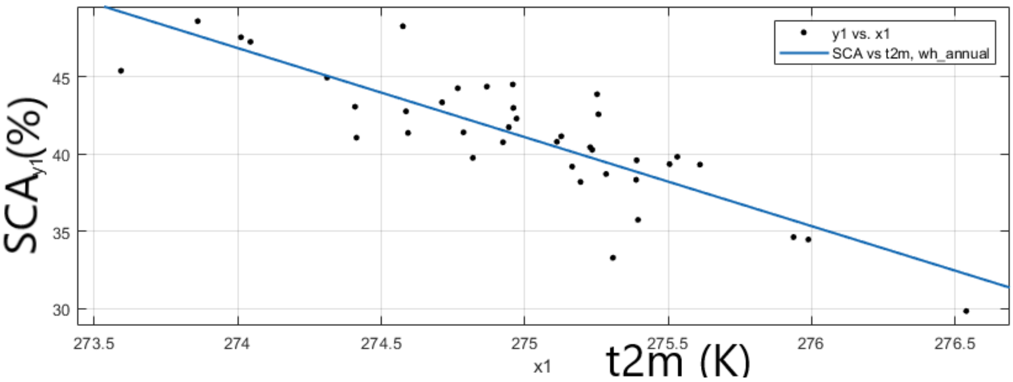

Figure 39 | SCA vs. t2m, WH_Annual

Linear Fit, 2 coefficients

$f(x) = p_1x + p_2$, where p_1 & p_2 are coefficients, $p_1 = -5.762$ & $p_2 = 1626$

How good the fit is?:		**Not good fit**	
R^2	Adjusted R^2	RMSE	SSE
0.705	0.6971	2.225	183.2

Table 32 | Regression Analysis for SCA Vs. t2m, WH_Annual

DJFM

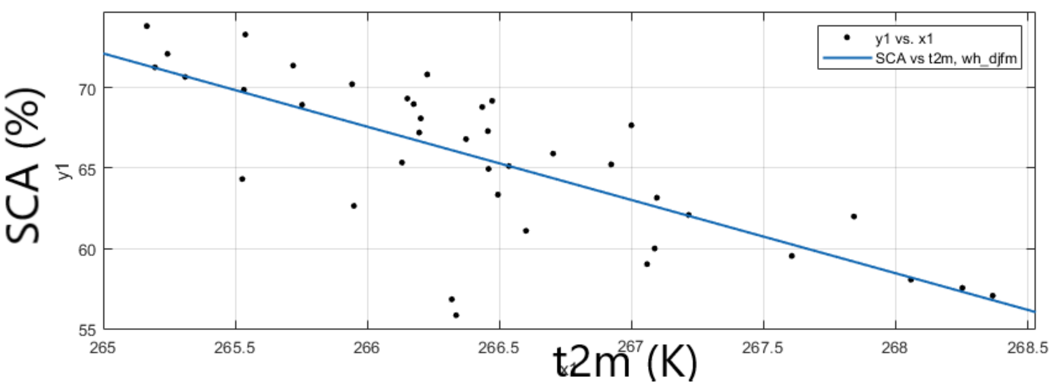

Figure 40 | SCA vs. t2m, WH_DJFM

Linear Fit, 2 coefficients

$f(x) = p_1x + p_2$, where p_1 & p_2 are coefficients, $p_1 = -4.558$ & $p_2 = 1280$

How good the fit is?:		Not good fit	
R^2	Adjusted R^2	RMSE	SSE
0.5618	0.5499	3.355	416.5

Table 33 | Regression Analysis for SCA Vs. t2m, WH_DJFM

JJAS

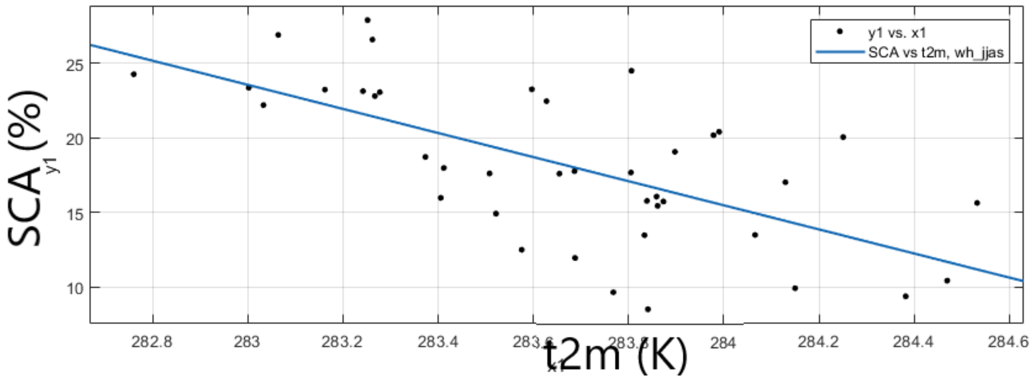

Figure 41 | SCA vs. t2m, WH_JJAS

Linear Fit, 2 coefficients

$f(x) = p_1x + p_2$, where p_1 & p_2 are coefficients, $p_1 = -8.072$ & $p_2 = 2308$

How good the fit is?:		Not good fit	
R^2	Adjusted R^2	RMSE	SSE
0.42	0.4047	3.998	607.5

Table 34 | Regression Analysis for SCA Vs. t2m, WH_JJAS

3.5.1.2.1.2. SCA vs Sf

Annual

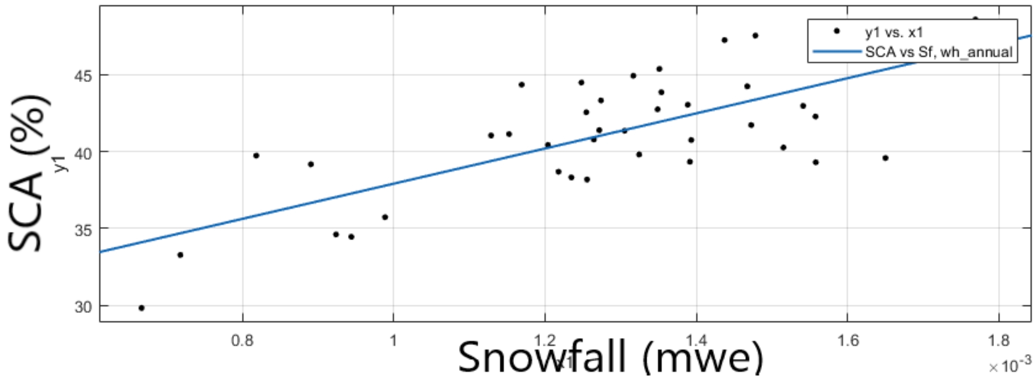

Figure 42 | SCA vs. Sf, WH_Annual

Linear Fit, 2 coefficients,

$f(x) = p_1x + p_2$, where p_1 & p_2 are coefficients, $p_1 = 1.143 \times 10^4$ & $p_2 = 26.49$

How good the fit is?:		**Not good fit**	
R^2	Adjusted R^2	RMSE	SSE
0.5373	0.5248	2.787	287.4

Table 35 | Regression Analysis for SCA Vs. Sf, WH_Annual

DJFM

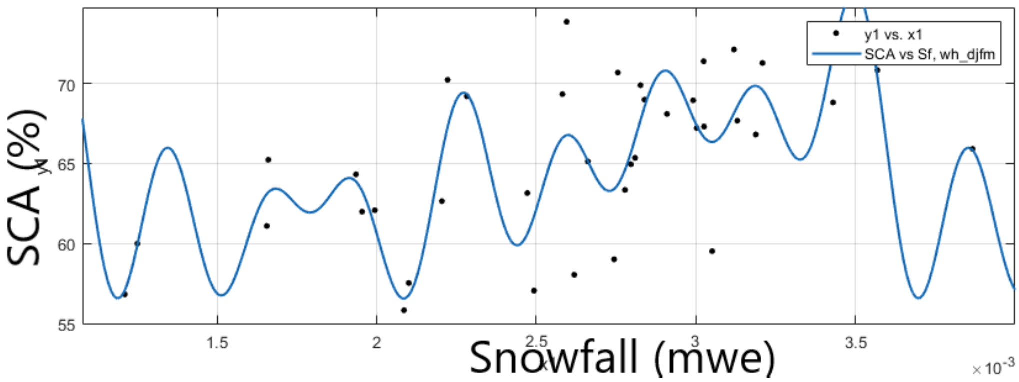

Figure 43 | SCA vs. Sf, WH_DJFM

Fourier 8 terms

Equation : $f(x) = a_0 + (a_1Cos(wx) + b_1Sin(wx)) + (a_1Cos(wx) + b_1Sin(wx)) + (a_2Cos(wx) + b_2Sin(wx)) + (a_3Cos(wx) + b_3Sin(wx)) +(a_4Cos(wx) + b_4Sin(wx)) + (a_5Cos(wx) + b_5Sin(wx)) + (a_6Cos(wx) + b_6Sin(wx)) + (a_7Cos(7wx) + b_7Sin(7wx)) + (a_8Cos(8wx) + b_8Sin(8wx))$, where a_0, b_0, …., a_8, b_8 & w are coefficients.

How good the fit is?:		**Not good fit**	
R^2	Adjusted R^2	RMSE	SSE
0.5907	0.2594	4.304	389

Table 36 | Regression Analysis for SCA Vs. Sf, WH_DJFM

3.5.1.3. TH

SCA with	**Annual**	**DJFM**	**JJAS**
T2m	-0.77* $P = 1.4 \times 10^{-7}$	-0.82* $P = 1.2 \times 10^{-8}$	-0.61* $P = 3.8 \times 10^{-5}$
Sf	0.52* $P = 8.1 \times 10^{-4}$	0.88* P = 0	0.91* P = 0

***statistically significant**

Table 37 | Spearman Correlation of SCA with Sf & t2m for TH

In TH region, SCA and t2m are strongly correlated during the annual & winter periods and moderately during JJAS period. During the monsoon period, a strong correlation exists between SCA & Sf and in contrast moderate correlation exists between SCA & t2m suggesting that for controlling SCA, t2m and sf both play the role but being sf on a lot higher side. In winter period, SCA is controlled by both t2m and sf significantly and during annual period, it is controlled by both being t2m on the higher side slightly.

3.5.1.3.1. Correlation Plots

3.5.1.3.1.1. SCA vs t2m

Annual

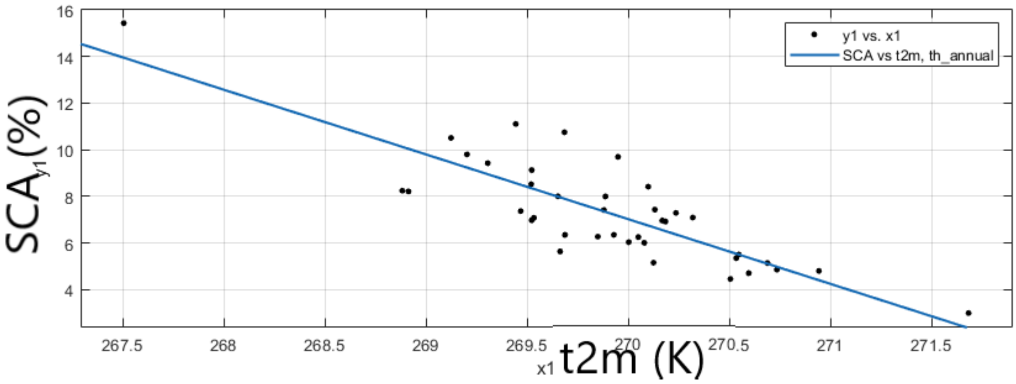

Figure 44 | SCA vs. t2m, TH_Annual

Linear Fit, 2 coefficients

$f(x) = p_1x + p_2$, where p_1 & p_2 are coefficients, p_1 = -2.774 & p_2 = 756.1

How good the fit is?:		**Not good fit**	
R^2	Adjusted R^2	RMSE	SSE
0.7027	0.6947	1.268	59.48

Table 38 | Regression Analysis for SCA Vs. t2m, TH_Annual

DJFM

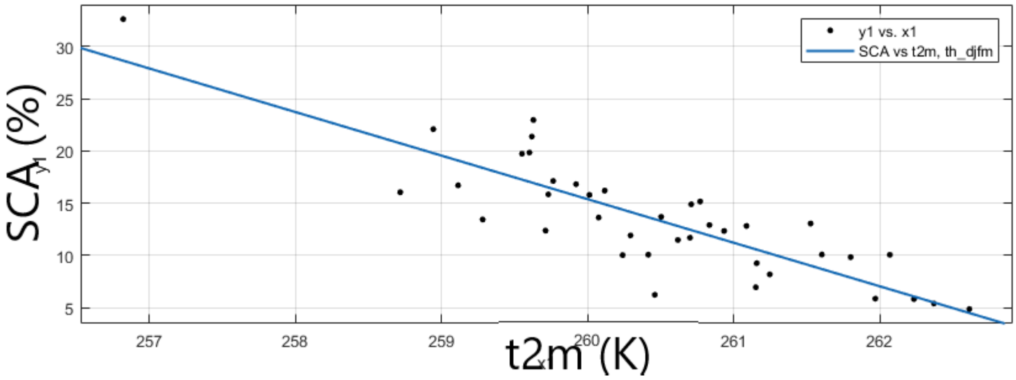

Figure 45 | SCA vs. t2m, TH_DJFM

Linear Fit, 2 coefficients

$f(x) = p_1x + p_2$, where p_1 & p_2 are coefficients, $p_1 = -4.173$ & $p_2 = 1100$

How good the fit is?:		Not good fit	
R^2	Adjusted R^2	RMSE	SSE
0.7242	0.7167	3.002	333.4

Table 38 | Regression Analysis for SCA Vs. t2m, TH_DJFM

JJAS

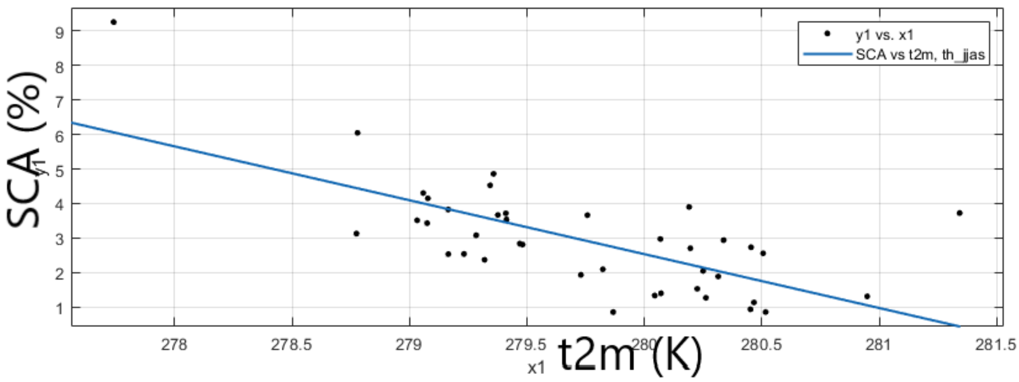

Figure 46 | SCA vs. t2m, TH_JJAS

Linear Fit, 2 coefficients

$f(x) = p_1x + p_2$, where p_1 & p_2 are coefficients, $p_1 = -1.561$ & $p_2 = 439.7$

How good the fit is?:		Not good fit	
R^2	Adjusted R^2	RMSE	SSE
0.4714	0.4575	1.161	51.24

Table 39 | Regression Analysis for SCA Vs. t2m, TH_JJAS

3.5.1.3.1.2. SCA vs Sf

Annual

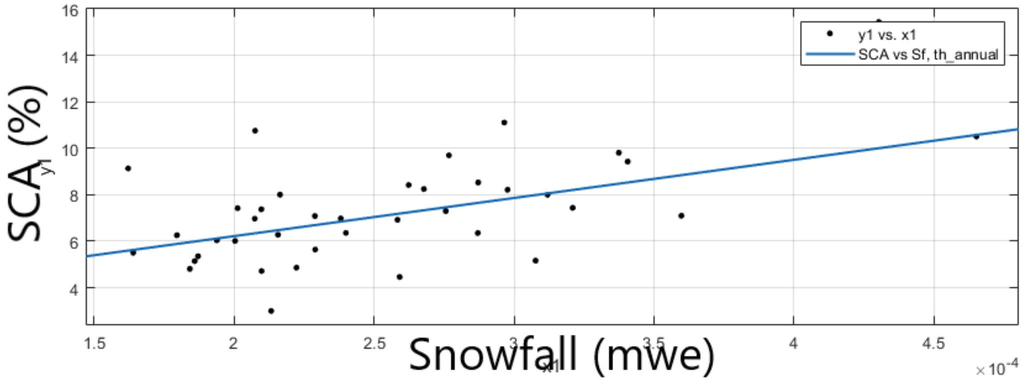

Figure 47 | SCA vs. Sf, TH_Annual

Linear Fit, 2 coefficients, Robust = Bisquare

$f(x) = p_1x + p_2$, where p_1 & p_2 are coefficients, $p_1 = 1.131$ & $p_2 = 7.119$

How good the fit is?:		Not good fit	
R^2	Adjusted R^2	RMSE	SSE
0.4706	0.4563	1.692	105.9

Table 39 | Regression Analysis for SCA Vs. Sf, TH_Annual

DJFM

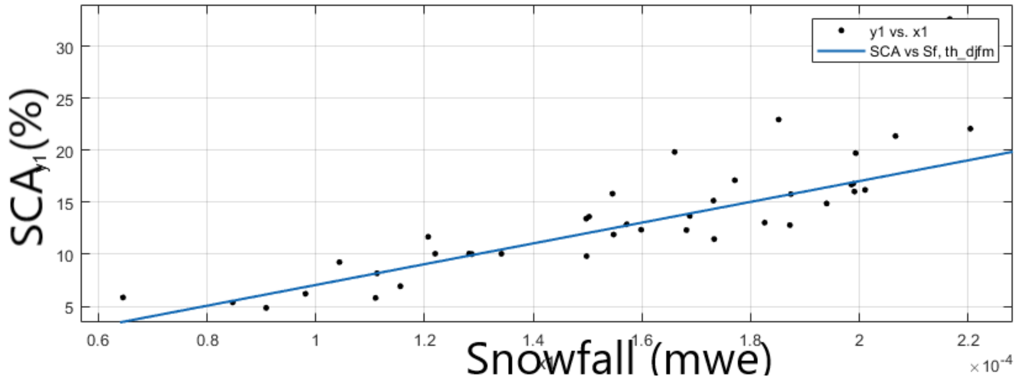

Figure 48 | SCA vs. Sf, TH_DJFM

Linear Fit, 2 coefficients, Robust = LAR

$f(x) = p_1x + p_2$, where p_1 & p_2 are coefficients, $p_1 = 9.986 \times 10^4$ & $p_2 = -2.931$

How good the fit is?:		Not good fit	
R^2	Adjusted R^2	RMSE	SSE
0.9728	0.9721	0.9419	32.82

Table 40 | Regression Analysis for SCA Vs. Sf, TH_DJFM

JJAS

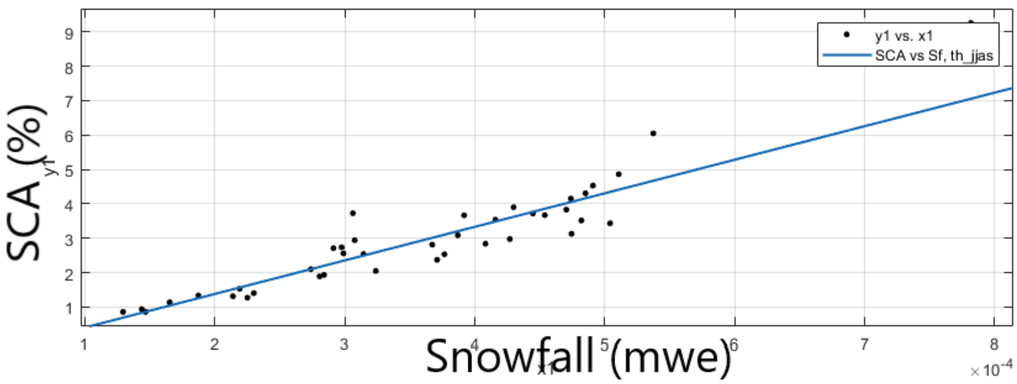

Figure 49 | SCA vs. Sf, TH_JJAS

Linear Fit, 2 coefficients, Robust = LAR

$f(x) = p_1x + p_2$, where p_1 & p_2 are coefficients, $p_1 = 9757$ & $p_2 = -0.5728$

How good the fit is?:		Not good fit	
R^2	Adjusted R^2	RMSE	SSE
0.9877	0.9873	0.1774	1.196

Table 41 | Regression Analysis for SCA Vs. Sf, TH_JJAS

4. Discussion

The annual and seasonal (winter & monsoon) snow cover variability and its response to main climatic variables were examined in depth over the NWH, WH & TH regions from 1979–2018. The ERA-5 reanalysis climatic data was used for the analysis due to its high spatio-temporal coverage. The study revealed several fluctuations in SCA annual & monsoon period yearly average with a significant decreasing trend from 1979-2018 with a rate of 0.35%/year & 0.07%/year in NWH respectively. The average annual temperature showed increasing trend in both NWH & WH with a rate of 0.018 °C/year & 0.016 °C/year respectively. The snowfall showed decreasing trends in annual and winter periods with a rate of 1.2×10^{-2} mm/year and 2.5×10^{-3} mm/year respectively in NWH where as in TH, it shows increasing trends in annual and monsoon period with a rate of 2.6×10^{-3} mm/year and 5.8×10^{-3} mm/year respectively. The snow depth showed decreasing trends in all 3 temporal scales in NWH, with a rate of 0.007 m/year, 0.008 m/year & 0.004 m/year in Annual, winter & monsoon periods respectively whereas increasing trend in TH for monsoon season was observed with a very small negligible rate. STR showed no trends for NWH region, but increasing trends in TH with a rate of 14273 J/m^2 year & 33607.75 J/m^2 year for Annual & monsoon period respectively. The SSHF showed decreasing trend in NWH region in the annual period with a rate of 7722.87 J/m^2 year and in TH region showed increasing trends in Annual & monsoon periods with a rate of 14428.95 J/m^2 year & 25868.83 J/m^2 year respectively. Also the Mann Kendall trend results were compared with ITA trend results. From ITA, Strong trend results were found for temperature annual scale for both low and high magnitude values in NWH & WH both study areas. So, to summarize our above discussions, we can conclude that for NWH region, among all periods, annual scale indicated a significant increasing temperature which may explain the decreasing SCA trend. The snow depth and snow cover area shows decreasing trend in annual and monsoon i.e., JJAS period which is due to decrease in trends of surface sensible heat flux and decreasing snowfall trends for annual scale only. For WH region, statistically significant increasing trends of temperature (t2m) was discovered only. For TH region, in JJAS, i.e., monsoon season, increasing trend of snow depth was found which is due to increase in SSHF and STR radiation trends and increase in snowfall trends, similar results were found from NASA articles**.** Mean of DJFM snowfall for all 3 study areas were calculated for 40 years and it was found that the snowfall in NWH is more than WH and then TH, which is due to the fact that as their winter climate dynamics are controlled by western disturbances and their influence on India from north decreases along southward and eastward direction. Similar results were also observed from (Yadav et al., 2021) [28]. The SCA trends were only observed in NWH region only for two temporal scales, i.e. decreasing SCA trends for annual and monsoon period and no trends were found for TH and for WH no significant trend square box was observed. Correlation analysis (Spearman correlation) revealed that the correlation coefficient between SCA & t2m are ranging from -0.77 to -0.82 for 40 years 1979-2018 for all study areas in annual scale which depicts increase of decrease in SCA for all study regions annually coincides with increase in t2m and decrease in snowfall can be verified by looking at their Interpolant plots where the plots are made for NWH region for SCA, t2m and snowfall respectively for annual scale here we can see for instance, for year 1995, SCA is decreasing, at the same time period, t2m is increasing and snowfall is decreasing as well. So, the correlation analysis for these multi spatial multi temporal study areas revealed that in NWH, for annual and monsoon periods, decrease in SCA is associated with t2m increasing and Sf decreasing as discussed earlier. In WH, for annual and winter period, same results are found as previous. In TH, the similar results came out to be true for all temporal scales, unlike NWH & WH. Then, model fitting was done for Sf, SCA and t2m time series as well as correlation plots of SCA, Sf and t2m for all temporal scales. This study revealed that the model that fits for snowfall with time for NWH region of DJFM time period; is a Fourier series with 7 terms equation, its R^2 value is moderate above 0.5, RMSE & SSE values are around zero, which shows least residual errors, so it seems from these statistical parameters, the curve seems like a good fit but since number of coefficients is more than 2, there are 7 terms with more than dozen coefficients, existence of these amount of coefficients is making adjusted R square very low compared to R square value and therefore this curve is not a good fit for prediction and then model fitting for SCA and Sf for NWH region for annual scale was done that came linear and is again not that good fit since SSE and RMSE values are very high even though R^2 value is moderately good, which gives a linear fit of minimal coefficients, which suggests why this time R^2 adjusted is around R^2 value. So, what this conveys is that for these model fits; correlation, p values & multiple correlation coefficient i.e. R^2, cannot be the only factors for predicting goodness of model fits. Seasonal ARIMA forecasting [29] can also be employed for better model fitting and predicting climatic variables for further years.

5. Conclusion

The Western-Central Section of Hindu Kush Himalayas comprises large amounts of snow cover and has diverse climatic conditions influenced by Western Disturbances during the winter period of the year. This study underlined the current scenario of snow cover over the NWH, WH & TH region so that the necessary steps could be taken accordingly for further research. A multi-parameter with multi-spatial-temporal analysis was carried out to understand the climate dynamics of Western-Central HKH especially for Sf, t2m, SCA, SDE, STR and SSHF. The correlation analysis was studied for SCA with temperature and snowfall over the study regions. The strength of inter-correlation between SCA and other meteorological parameters was revealed. It was observed that SCA decreased with an increase in temperature and decreased snowfall and vice versa for most of the multi spatial-temporal study regions except for winter season of NWH & monsoon season of WH where non-significant spearman correlation was observed. The model fitting of climatic variables among them and with temporal scale was computed via regression that revealed for most of spatial-temporal areas of our study regions, the 60% models are Fourier series with more than 6 terms and others are sum of sine series with more than 6 terms for Sf, SCA & t2m time series plots whereas 70% models are linear fit for correlation plots of SCA with Sf & t2m respectively. It was discovered that there is an increasing trend of surface temperature, the existence of decreasing trend of snow cover with the loss of back radiation & heat flux of Earth's emission which affects snowfall in Northwestern part of Himalayas since last 40 years due to global warming, that would create enough disaster risks in India such as floods, tsunamis and other natural disasters for future due to ongoing snow cover melt and most importantly the Himalayas are the most climatically dynamic and sensitive parts of the world on which millions of lives and livelihoods are dependent, such as small & medium-sized businesses would be severely impacted. India is a tropical country that is still in the developing phase and is struggling with the effects of climate change. There is an essential need to do further research, and develop & implement mitigation policies to make India climate-resilient.

6. References

1. Viviroli, D., Dürr, H. H., Messerli, B., Meybeck, M., & Weingartner, R. (2007). Mountains of the world, water towers for humanity: Typology, mapping, and global significance. *Water resources research*, *43*(7).
2. Chen, X., Long, D., Liang, S., He, L., Zeng, C., Hao, X., & Hong, Y. (2018). Developing a composite daily snow cover extent record over the Tibetan Plateau from 1981 to 2016 using multisource data. *Remote Sensing of Environment*, *215*, 284-299.
3. Sicart, J. E., Pomeroy, J. W., Essery, R. L. H., & Bewley, D. (2006). Incoming longwave radiation to melting snow: observations, sensitivity and estimation in northern environments. *Hydrological processes*, *20*(17), 3697-3708.
4. Brown, R. D. (2000). Northern Hemisphere snow cover variability and change, 1915–97. *Journal of climate*, *13*(13), 2339-2355.
5. Hosaka, M., Nohara, D., & Kitoh, A. (2005). Changes in snow cover and snow water equivalent due to global warming simulated by a 20km-mesh global atmospheric model. *Sola*, *1*, 93-96.
6. Singh, D. K., Gusain, H. S., Mishra, V., & Gupta, N. (2018). Snow cover variability in North-West Himalaya during last decade. *Arabian Journal of Geosciences*, *11*(19), 1-12.
7. Shafiq, M. U., Ahmed, P., Islam, Z. U., Joshi, P. K., & Bhat, W. A. (2019). Snow cover area change and its relations with climatic variability in Kashmir Himalayas, India. *Geocarto International*, *34*(6), 688-702. Bednorz, E. (2004). Snow cover in eastern Europe in relation to temperature, precipitation and circulation. *International Journal of Climatology: A Journal of the Royal Meteorological Society*, *24*(5), 591-601.
8. Bednorz, E. (2004). Snow cover in Eastern Europe in relation to temperature, precipitation and circulation. *International Journal of Climatology: A Journal of the Royal Meteorological Society*, *24*(5), 591-601.
9. Trenberth, K. E., Jones, P. D., Ambenje, P., Bojariu, R., Easterling, D., Klein Tank, A., ... & Zhai, P. (2007). Observations. Surface and atmospheric climate change. Chapter 3.
10. Bhutiyani, M. R., Kale, V. S., & Pawar, N. J. (2007). Long-term trends in

maximum, minimum and mean annual air temperatures across the Northwestern Himalaya during the twentieth century. *Climatic Change*, *85*(1), 159-177.

11. Shekhar, M. S., Chand, H., Kumar, S., Srinivasan, K., & Ganju, A. (2010). Climate-change studies in the western Himalaya. *Annals of Glaciology*, *51*(54), 105-112.
12. Niederer, P., Bilenko, V., Ershova, N., Hurni, H., Yerokhin, S., & Maselli, D. (2008). Tracing glacier wastage in the Northern Tien Shan (Kyrgyzstan/Central Asia) over the last 40 years. *Climatic Change*, *86*(1), 227-234.
13. Shekhar, M. S., Chand, H., Kumar, S., Srinivasan, K., & Ganju, A. (2010). Climate-change studies in the western Himalaya. *Annals of Glaciology*, *51*(54), 105-112.
14. Hansen, J., & Nazarenko, L. (2004). Soot climate forcing via snow and ice albedos. *Proceedings of the national academy of sciences*, *101*(2), 423-428.
15. Menon, S., Koch, D., Beig, G., Sahu, S., Fasullo, J., & Orlikowski, D. (2010). Black carbon aerosols and the third polar ice cap. *Atmospheric Chemistry and Physics*, *10*(10), 4559-4571.
16. Zurick, D., & Pacheco, J. (2006). *Illustrated atlas of the Himalaya*. India Research Press.
17. Negi, H. S., Kulkarni, A. V., & Semwal, B. S. (2009). Estimation of snow cover distribution in Beas basin, Indian Himalaya using satellite data and ground measurements. *Journal of Earth System Science*, *118*(5), 525-538.
18. Kaur, R., Saikumar, D., Kulkarni, A. V., & Chaudhary, B. S. (2009). Variations in snow cover and snowline altitude in Baspa Basin. *Current Science (00113891)*, *96*(9).
19. Ming, J., Wang, Y., Du, Z., Zhang, T., Guo, W., Xiao, C., ... & Yang, W. (2015). Widespread albedo decreasing and induced melting of Himalayan snow and ice in the early 21st century. *PLoS One*, *10*(6), e0126235.
20. Searle, M. P., & Searle, M. (2013). *Colliding continents: a geological exploration of the Himalaya, Karakoram, and Tibet*. Oxford University Press.
21. Mann, H. B. (1945). Nonparametric tests against trend. *Econometrica: Journal of the econometric society*, 245-259.
22. Kendall, M. G. (1948). Rank correlation methods.
23. Hamed, K. H. (2011). The distribution of Kendall's tau for testing the significance of cross-correlation in persistent data. *Hydrological sciences*

journal, *56*(5), 841-853.

24. Sen, P. K. (1968). Estimates of the regression coefficient based on Kendall's tau. *Journal of the American statistical association*, *63*(324), 1379-1389.
25. Şen, Z. (2012). Innovative trend analysis methodology. *Journal of Hydrologic Engineering*, *17*(9), 1042-1046.
26. Elouissi, A., Şen, Z., & Habi, M. (2016). Algerian rainfall innovative trend analysis and its implications to Macta watershed. *Arabian Journal of Geosciences*, *9*(4), 303.
27. Zakwan, M., & Ahmad, Z. (2021). Trend analysis of hydrological parameters of Ganga River. *Arabian Journal of Geosciences*, *14*(3), 1-15.
28. Choudhury, A., Yadav, A. C., & Bonafoni, S. (2021). A Response of Snow Cover to the Climate in the Northwest Himalaya (NWH) Using Satellite Products. *Remote Sensing*, *13*(4), 655.
29. Dimri, T., Ahmad, S., & Sharif, M. (2020). Time series analysis of climate variables using seasonal ARIMA approach. *Journal of Earth System Science*, *129*(1), 1-16.